DocuSign Envelope ID: FF917FA4-BEA0-4E08-96D0-A9016C337F14

COMPARISON OF AIRWAY COLLAPSIBILITY IN CHILDREN WITH SIGNS AND SYMPTOMS OF SLEEP DISORDERED BREATHING USING SUBMENTAL ULTRASOUND

by

CRAIG J. MADISON, D.M.D.

Submitted in partial fulfillment of the requirements for the degree of
Master of Science in Dentistry

Thesis Advisor: Mark Hans, D.D.S, M.S.D.
Committee Members:
Juan Martin Palomo D.D.S., M.S.D.
Denise Dewald M.D.

Case Western Reserve University
School of Dental Medicine
Department of Orthodontics
January 14th, 2022

DocuSign Envelope ID: FF917FA4-BEA0-4E08-96D0-A9016C337F14

DEDICATION

This work is dedicated to my loving wife, Lindsey, who has supported me throughout the entirety of completing this thesis. You did not hesitate to uproot your life and move to Cleveland with me when I started residency, and without you here, it would have been a much more difficult process. You were my rock through the ups and downs. I would also like to dedicate this work to my parents, without whom I would not be where I am today. You pushed me to achieve success and were always there for me when I needed advice.

DocuSign Envelope ID: FF917FA4-BEA0-4E08-96D0-A9016C337F14

ACKNOWLEDGEMENTS

Many thanks to Dr. Mark Hans, who played a major role in my decision to come to CWRU for residency. You inspired me to take on a thesis project looking at data on the cutting edge of sleep medicine. Your support through the ups and downs of embarking on such a project was unwavering. I am sure you will inspire more residents at CWRU to conduct thesis projects that build on this one.

To Dr. Juan Martin Palomo, you were my day-to-day contact who was always open to help me with questions that arose as I completed this project. Your leadership in navigating the program through a pandemic did not go unnoticed. You kept us all learning through months of lock down, and for that I am very grateful.

To Dr. Denise Dewald, for imparting on me your expertise in the anatomy of the upper airway. You were very gracious for always taking time out of your schedule to help me learn the intricacies of the upper airway that only experts in the field know. I truly feel like I gained knowledge from you that I will take with me into practice for years to come.

To my CWRU orthodontic family – co-residents, faculty, and staff – you all played such an instrumental role in molding me into the

DocuSign Envelope ID: FF917FA4-BEA0-4E08-96D0-A9016C337F14

orthodontist that I have become. To my co-residents, we have made some amazing memories both inside and out of the clinic, and I am sure we will make many more in the years to come. To the faculty, I cannot thank you enough for your volunteer hours put in to teach us orthodontics. I strive to be as good of an orthodontist as all of you in the future. To the staff, your hard work and dedication kept the clinic running, and without you we would not have had such a great clinic experience.

Last, to my wife Lindsey, parents, and sister Bethany. You have all played your own roles in the person and orthodontist I have become. You have all supported me in your own ways and were always there when I needed you. I am beyond grateful for all of you.

DocuSign Envelope ID: FF917FA4-BEA0-4E08-96D0-A9016C337F14

COMPARISON OF AIRWAY COLLAPSIBILITY IN CHILDREN WITH SIGNS AND SYMPTOMS OF SLEEP DISORDERED BREATHING USING SUBMENTAL ULTRASOUND

Abstract

by

CRAIG JOSEPH MADISON

Introduction: The purpose of this study was to use submental ultrasound data to examine airway collapse observed in children with signs and symptoms of sleep disordered breathing (SDB). The amount and pattern of airway collapse was compared amongst subjects, as well as between subjects and adults with and without OSA.

Methods: In this retrospective study, 18 subjects were included. Data collected for each patient included BMI, gender, age, Pediatric Sleep Questionnaire (PSQ) answers and score, along with submental ultrasound scan data, which included the amount of lateral airway collapse. The amount and pattern of airway collapse was compared amongst subjects, as well as between subjects and adults with and without OSA.

DocuSign Envelope ID: FF917FA4-BEA0-4E08-96D0-A9016C337F14

Results: Mean airway collapse was calculated at Velum 8.96% ± 9.62%, Oropharynx 13.25% ± 10.44%, Tongue Base 16.39% ± 14.70%, and Epiglottis 11.25% ± 7.95%. The amount of lateral airway collapse varied widely across the sample. Lateral airway collapse was not uniform across the upper airway. Four of the 18 ultrasound scans had been repeated as part of orthodontic screening to confirm the patient's risk assessment. Total amount of collapse was similar for the repeated scans, but the location of greatest collapse differed, making repeatability questionable. The patients at highest risk for SDB according to the PSQ did not necessarily have high amounts of lateral airway collapse. The mean amounts of airway collapse found in this sample were considerably less than that of patients even without OSA in Shu et al's 2013 study.

Conclusion: Submental ultrasound provides a way to image the airway in a non-invasive, radiation-free way. This study found that collapse is not uniform across the upper airway and that the amount and pattern of airway collapse varied among each subject. High risk on the PSQ did not necessarily relate to high lateral collapse of the airway. Repeatability of results over multiple scans is questionable, as slight differences in patient positioning can lead to inaccuracies in the software's division of the airway into four regions.

DocuSign Envelope ID: FF917FA4-BEA0-4E08-96D0-A9016C337F14

TABLE OF CONTENTS

DEDICATION ii

ACKNOWLEDGEMENTS….....iii

ABSTRACT.....v

REVIEW OF THE LITERATURE 1

LIT REVIEW REFERENCES.....34

STATEMENT OF THE THESIS.....40

MANUSCRIPT FOR PUBLICATION.....41

MANUSCRIPT REFERENCES. 67

APPENDICES……...70

A. IRB APPROVAL……70

B. ABBREVIATION KEY……71

C. AIRSPACE CONTRACTION SUMMARY PER SUBJECT……..72

D. GRAPH OF AIRSPACE CONTRACTION PER SUBJECT……81

E. AIRSPACE CONTRACTION RAW DATA PER SUBJECT……88

DocuSign Envelope ID: FF917FA4-BEA0-4E08-96D0-A9016C337F14

LIST OF TABLES

Table I: Airway Collapse by Subject……..……60

Table II: Comparison of collapse to Shu et al. 2013…..……61

LIST OF FIGURES

Figure 1: AmCAD-UO ultrasound system diagram……..…62

Figure 2: Patient positioning in AmCAD-UO unit……..……62

Figure 3: Resulting image with ultrasound probe in position……...…63

Figure 4: Ultrasound tablet and probe image……..…63

Figure 5: Depiction of velum, oropharynx, tongue base, epiglottis..64

Figure 6: Airway at normal breathing and Muller maneuver……..64

Figure 7: Airway collapse for subjects 1-9……..……...…65

Figure 8: Airway collapse for subjects 10-18……..……...…65

Figure 9: Airway collapse for repeated scans……..……...…66

Figure 10: retropalatal and retroglossal comparison..……..……66

DocuSign Envelope ID: FF917FA4-BEA0-4E08-96D0-A9016C337F14

REVIEW OF THE LITERATURE

Introduction

Sleep disordered breathing and its spectrum – from primary snoring to obstructive sleep apnea – affects both adults and children. This literature will provide a comprehensive overview of sleep disordered breathing, sleep apnea, pharyngeal anatomy, and current screening/diagnostic techniques for the condition. The review will end with the relevance of sleep apnea to the field of orthodontics.

Obstructive Sleep Apnea Overview

Sleep apnea, by definition, includes the cessation of breathing during sleep (apneas), as well as reduction in breathing during sleep (hypopneas)(1). Sleep apnea can be further broken down into two categories – central sleep apnea (CSA) and obstructive sleep apnea (OSA). The former is the result of decreased neural impulses directly from the central nervous system to the muscles of the respiratory pump. This results in a marked decrease in the drive to breathe, causing repetitive episodes of central apnea (1). The latter – obstructive sleep apnea – is far more common to be encountered in clinical practice and will be the focus of this literature review.

DocuSign Envelope ID: FF917FA4-BEA0-4E08-96D0-A9016C337F14

Obstructive sleep apnea, as indicated by its title, is caused by obstruction of the upper airway during sleep. This airway obstruction – the result of narrowing or "collapse" of the upper respiratory passages – leads to a decrease or complete cessation of breathing (hypopnea or apnea, respectively) (2). These breathing disruptions lead to repeated arousals that affect sleep continuity, thus depriving the individual of deep, restful sleep (2). Expectedly, this leads to chronic fatigue and/or daytime sleepiness. Further, adverse health conditions such as hypertension, congestive heart failure, cardiac arrhythmias, and depression are associated with obstructive sleep apnea (2,3). Obstructive sleep apnea effects people of all ages. OSA in children may have a different clinical presentation than adults – with an apparent negative impact on cognitive development, performance in school, and behavior (4). Pediatric obstructive sleep apnea will be described in detail in its own section of this literature review.

The exact prevalence of OSA is not known, but studies have estimated that 2-14% of the general population has some degree of obstructive sleep apnea (2). Prevalence is very much influenced by age and obesity. OSA effects men approximately three times more than females (5). Even so, it is believed that the actual prevalence of OSA is greater than most estimates as many cases go undiagnosed due to

DocuSign Envelope ID: FF917FA4-BEA0-4E08-96D0-A9016C337F14

under recognition by practitioners (5). The diagnostic gold standard for obstructive sleep apnea in both adults and children is polysomnography (PSG). However, PSG is expensive, invasive, and time consuming, contributing to this underreporting of OSA in the general population. As such, it is of the utmost importance to screen for obstructive sleep apnea in clinical practice and refer for diagnosis whenever possible.

The front-line treatment for obstructive sleep apnea in adults in Continuous Positive Airway Pressure (CPAP) (5). For those who cannot tolerate or do not respond to CPAP, oral appliances that advance the mandible or manipulate tongue posture may be used (5). Other approaches, such as orthognathic surgery to advance both the maxilla and mandible may be considered, but only when an underlying skeletal discrepancy indicates the need for orthognathic surgery (5). Novel treatments such as hypoglossal nerve stimulation show promise for adding new treatment options and improving treatment modalities and care in the future (2). Treatment of OSA in the pediatric population differs from that of the adult population, and will be discussed in detail in its own section of this literature review. Along with a detailed discussion of current knowledge on pediatric sleep disordered breathing (SDB) and OSA, the remainder of this literature review will also discuss pharyngeal anatomy in detail, current screening and diagnostic techniques for

DocuSign Envelope ID: FF917FA4-BEA0-4E08-96D0-A9016C337F14

obstructive sleep apnea, and the relevance of obstructive sleep apnea to the orthodontic specialty.

Sleep Disordered Breathing and Obstructive Sleep Apnea in the Pediatric Population

As mentioned above, obstructive sleep apnea effects people of all age groups. Pediatric obstructive sleep apnea is a subset of a spectrum of conditions known as pediatric sleep-disordered breathing (SDB) (6). SDB encompasses of range of conditions spanning from snoring, to upper airway resistance syndrome, to obstructive sleep apnea (6). Of these, habitual snoring and OSA are the most common presentations of sleep disordered breathing. Both presentations of SDB have been associated with negative effects on neurocognitive and behavioral developments, along with impairment in memory, attention, and social interactions (6). Habitual snoring has been estimated at 1.5-14.8% in the pediatric population, where pediatric OSA is estimated at 1-4% of the population (general population is estimated at 2-14%) (6). Such variation in estimates is largely due to the wide variety of screening and diagnostic tools available to practitioners, with varying definitions of habitual snoring and OSA risk assessment (7). A systematic review by Lumeng in 2008 looked at rates of SDB and pediatric OSA prevalence

DocuSign Envelope ID: FF917FA4-BEA0-4E08-96D0-A9016C337F14

and found that parent-reported "always" snoring ranged from 1.5-6%, parent reported apneic events during sleep from 0.2-4%, SBD prevalence of 4-11% based on parent reported answers to a questionnaire, OSA diagnosed at 1-4%, and snoring by any definition of 7.45% (7). The study reported that snoring is frequently associated with OSA, and patients who initially fall on the primary snoring end of the SDB spectrum may be at risk for development of OSA with age or weight gain (7). They also reported that almost all individuals with pediatric OSA have habitual snoring (7). Even though there is wide variability in reported rates of SDB and OSA in the pediatric population, it is clear that OSA and SDB do exist in the pediatric population and must not be ignored. Further, it is evident that primary snoring - even though on the low end of the SDB spectrum – must not be downplayed as it may be the primary clinical manifestation of pediatric OSA. In fact, in their guidelines on managing pediatric OSA the American Academy of Pediatric Sleep Physicians state, "If they snore, you must do more" (5). Orthodontists are in a prime position to screen for pediatric OSA and thus are obligated to do so. Because obstructive sleep apnea is the most severe condition of the sleep disordered breathing spectrum, and that snoring may be indicative of pediatric OSA, the remainder of this section of the literature review will focus on pediatric OSA.

DocuSign Envelope ID: FF917FA4-BEA0-4E08-96D0-A9016C337F14

Pediatric obstructive sleep apnea has a different clinical presentation than that of adults. This difference in clinical presentation was first described in 1981 when Guilleminault et al. published a review of 50 pediatric patients with OSA (8). They emphasized that compared to adults – where the main symptom of OSA is excessive daytime sleepiness – pediatric OSA is characterized less by daytime sleepiness and more by disturbed nocturnal sleep (9). This disturbed sleep negatively affects the patient's neurocognitive development, which leads to behavioral problems, struggles in school, hyperactivity, depression, insomnia, and psychiatric problems (10). Beyond the physical and mental health effects of SDB in the child, disrupted sleep can be a major psychological stressor for children and their families (9). Early diagnosis of pediatric OSA may reduce the occurrence of neurocognitive and systemic complications over time, although the diagnosis is often made too late due to under recognition by practitioners (11).

The underlying etiology of Pediatric OSA and sleep disordered breathing is complex, and although adult and pediatric OSA have similar etiologic factors, there are some key differences. For example, lymphoid hyperplasia and growth related changes of the upper airway contribute to presence and resolution of pediatric OSA, respectively. This

DocuSign Envelope ID: FF917FA4-BEA0-4E08-96D0-A9016C337F14

is clearly not seen in adult OSA as growth is complete in these patients (5). However, as with adult OSA, impaired neuromuscular tone underlies the upper airway collapse seen in pediatric OSA. In a 2003 study, Gozal and Burnside directly measured upper airway collapse in children with and without sleep disordered breathing by measuring the amount of airway collapse that occurs when the upper airway is anesthetized (to simulate sleep conditions) (12). They found that children with sleep disordered breathing do in fact show greater airway collapsibility than those without SDB (12). A detailed description of the pharyngeal airway anatomy and how muscular tone affects airway collapse will be covered in a separate section of this literature review.

Risk factors for pediatric OSA include adenotonsillar hypertrophy, obesity, allergic rhinitis, prematurity, asthma, environmental exposure to smoking, and other less frequent factors such as craniofacial anomalies, and neuromuscular disorders (11). Adenotonsillar hypertrophy is the most common condition associated with pediatric OSA (13). However, it is important to note that not all patients with large tonsils are affected with OSA, and thus is it proposed that isolated tonsillar hypertrophy is not sufficient to diagnose pediatric OSA (11). Obesity is becoming more prominent as a risk factor for OSA as years past. In their 2019 review on pediatric OSA, Savini et al reported that obesity plays a predominant

DocuSign Envelope ID: FF917FA4-BEA0-4E08-96D0-A9016C337F14

role in developing OSA in adolescence, due to weight gain in some patients during this period. They also reported that less than 50% of obese children undergoing adenotonsillectomy have complete resolution of their sleep disordered breathing. Clearly, obesity is a major risk factor in the development of pediatric OSA.

The first line of treatment for pediatric OSA is adenotonsillectomy, as enlarged tonsils are the leading contributor to pediatric OSA (14). In fact, tonsillectomy is one of the most common pediatric surgical procedures performed (15). Removal of the tonsils and adenoids directly increases the volume of the upper airway, making obstruction less likely to occur, through simple "debulking" of the airway (4). Due to risk involved in the procedure, some debate exists between surgical intervention versus watchful waiting. A 2013 randomized controlled trial by Marcus et al. comparing surgery and observation found that 76% of patients who underwent adenotonsillectomy had resolution of OSA, while just 46% of those who underwent a period of watchful waiting had resolution of OSA (16). A Cochrane review of the literature concluded that there is moderate quality evidence that adenotonsillectomy provides benefits in terms of quality of life, OSA symptoms, and behavior, however it found no difference in neurocognitive performance compared to watchful waiting (17). Studies have shown that residual

DocuSign Envelope ID: FF917FA4-BEA0-4E08-96D0-A9016C337F14

OSA exists in up to 25%-40% of pediatric patients after adenotonsillectomy (18). In their review on alternative treatment options to adenotonsillectomy, Rana et al. recommend continuous positive airway pressure (CPAP) as the first-line treatment to pediatric OSA cases refractory to adenotonsillectomy (18). For patients who cannot tolerate CPAP, other treatment options include weight loss, positional therapy, orthodontic procedures such as rapid maxillary expansion and mandibular advancement with removable or fixed-functional appliances (18). For those with mild OSA, treatment with intranasal steroids and/or montelukast may be considered (19).

Pharyngeal Airway Anatomy and its Implication in OSA

Increased collapsibility of the upper airway is the main etiologic factor underlying both pediatric and adult OSA (5). Impaired neuromuscular tone of the muscles of the pharynx directly influences this collapsibility (5). This section of the literature review will describe the muscles of the pharynx, their role in maintaining a patent airway, and how dysfunction of these muscles is related to airway collapse and OSA. This section will also touch on hard tissue anatomical considerations in OSA.

DocuSign Envelope ID: FF917FA4-BEA0-4E08-96D0-A9016C337F14

Not including the soft palate, the pharynx is a tube-like structure that is composed of six muscles – three constricting, external circular muscles (the superior, middle, and inferior constrictors), and three dilating, internal longitudinal muscles (the stylopharyngeus, palatopharyngeus, and salpingopharyngeus) (20). Of these six, all but one – the stylopharyngeus – have origins and insertions in the internal surface of the pharynx. The stylopharyngeus has its origin outside the pharynx, the styloid process, and then penetrates the constrictor muscles to its insertion in the internal pharynx (20). The extensive interconnections between these muscles mean that they form a functional unit; each muscles activity affects the tension and orientation of the other muscles (20).

In a 2020 study, Choi et al examined the topography and variations of stylopharyngeus (STP) and superior constrictor (SC) muscles in 42 adult cadavers. They found that both muscles have multiple anatomic variations (20). For example, one variation of stylopharyngeus was found to have an accessory bundle that runs longitudinally. The authors suggested that this variant may increase the STP's ability to shorten and elevate the pharynx upon contraction. Another variant of STP was located further behind the posterior wall of the pharynx, and the authors suggested that this variant may allow for greater increase in

DocuSign Envelope ID: FF917FA4-BEA0-4E08-96D0-A9016C337F14

the anterior posterior diameter of the oropharynx. Further, they found that the superior constrictor occasionally had fibers that ran longitudinally, which would contribute to the function of the internal muscles (stylopharyngeus, palatopharyngeus, and salpingopharyngeus) (20). Overall, this study supports the idea that different anatomical variations of the pharyngeal musculature may contribute to differences in total amount of airway collapse in OSA as well as in the pattern of collapse. A study by Fukino et al in 2018 examined the anatomical significance of the morphology of the palatopharyngeus muscle in terms of velopharyngeal closure (21). They described the Palatopharyngeus muscle as having three parts – a lateral part, superomedial part, and inferior part. They postulated that contraction of the superomedial part affects the medial protrusion of the lateral pharyngeal wall, and thus may be implicated in lateral collapse of the pharynx (21).

Another study by Sakamoto in 2009 aimed to classify the pharyngeal muscles based on innervation (22). Through careful dissection, they classified the pharyngeal muscles into 4 groups based on innervation. The first group includes the stylopharyngeus and glossopharyngeal portion of the superior constrictor, and are all innervated by the glossopharyngeal nerve. The second group which

DocuSign Envelope ID: FF917FA4-BEA0-4E08-96D0-A9016C337F14

consists of the other parts of the superior constrictor, salpingopharyngeus, and palatopharyngeus, and the third group which solely contains the middle constrictor, are all innervated by the pharyngeal plexus. The fourth group, the inferior constrictor, has innervation consisting of the pharyngeal plexus and external and recurrent laryngeal nerves (22). Interestingly, they found anomalous nerve bundles and anatomic variations within the first, second and third groups. The authors suggest that these anatomical variations seem to influence pharyngeal functions (22), and thus may play a role in varying amounts of neuromuscular tone observed in OSA patients.

The normal function of the pharyngeal muscles is key in maintaining a patent airway, and disturbance in function of the pharyngeal muscles is often seen in those with obstructive sleep apnea. In a 1977 study, Guilleminault et al used a fiberoptic endoscope in combination with electrodes implanted into pharyngeal muscles to attempt to locate the most common area of airway collapse as well as to identify which muscles are involved in collapse. The subjects were monitored during wakefulness and sleep. The study found that during sleep-induced apnea, patients with obstructive sleep apnea showed significant decrease or complete disappearance of electromyogram (EMG) activity in the palatoglossus, palatopharyngeus, genioglossus,

DocuSign Envelope ID: FF917FA4-BEA0-4E08-96D0-A9016C337F14

superior and middle constrictors, and stylopharyngeus. EMG activity was not decreased in the stylohyoid, cricopharyngeus, or inferior constrictor muscles (23). Based on this, the authors concluded that the obstruction observed during sleep involves the absence of the activity of the pharyngeal dilators needed to counteract the loads abruptly imposed by intrathoracic negative pressure changes. Using the fiberoptic endoscope, the authors also concluded that the primary site of obstruction is supraglottic, in the oropharynx, and that the posterolateral walls of the pharynx were the first to invaginate on collapse (23). They argue that the pharyngeal walls are the initiator of the obstructive phenomenon, not the tongue (23). Further, they put forward a "pharyngeal tent" hypothesis as a way to describe the muscles of the upper airway. They suggest that the superior and middle constrictors act as the roof of the tent, with the stylopharyngeus acting as the support to keep the tent up, as its fibers insert into the pharynx and spread widely beneath the mucous membrane. Contraction of the stylopharyngeus draws the sides of the upper pharynx cranially and laterally, increasing the transverse diameter of the pharynx (23). As so, dysfunction of the stylopharyngeus muscle would decrease the ability of the patient to maintain a patent airway in the transverse dimension.

DocuSign Envelope ID: FF917FA4-BEA0-4E08-96D0-A9016C337F14

Another interesting consideration in pharyngeal anatomy is the hyolaryngeal complex and its relation to the pharyngeal musculature; the larynx is coupled to the pharynx via the hyoid apparatus. A 1947 study by Mitchinson and Yoffey examined the amount of displacement of the larynx, hyoid bone and tongue during respiration. They used radiographic imaging to measure the position of the hyolaryngeal complex at the extremes of inspiration and expiration in apparently normal human subjects. They found that in 5 subjects there was elevation of the larynx, in 4 subjects descent of the larynx, and in the remaining 14 subjects no appreciable vertical displacement. They suggest that non-descent of the larynx during inspiration is due to contraction of the suprahyoid muscles as well as the stylopharyngeus and thyrohyoid muscles (24). They describe the trachea as being "slung from the base of the skull" by these muscles. They also found that the hyoid bone underwent a similar vertical displacement as the larynx. In all, this study shows that there does exist a variation in muscular tone in the general population, as the larynx was displaced by varying amounts and direction amongst different subjects (24). From this study one might extrapolate that those with OSA and decreased muscle tone would show increased movement of the hyolaryngeal complex on inspiration. In fact, this exact idea was explored in a 2019 study by Tong et al. (25).

DocuSign Envelope ID: FF917FA4-BEA0-4E08-96D0-A9016C337F14

They examined 34 awake patients via MRI to quantify the amount of tracheal displacement in those with and without obstructive sleep apnea. They hypothesized that those with OSA would show greater tracheal displacement than those without, and argued that caudal displacement of the larynx in those with OSA would help to "stiffen" the pharyngeal dilators and aid in maintaining airway patency (25). It's alternatively possible that this excessive movement of the trachea is indicative of weakness of the longitudinal pharyngeal muscles, such as stylopharyngeus. Regardless, their study confirmed that those with OSA show a greater inferior displacement of the trachea than those without. They suggest that the amount of tracheal displacement may be a novel way to screen for and predict severity of OSA (25).

A 1979 study by Rood et al. examined the anatomy of the tonsillar bed in fetuses, and postulated regarding the function of these muscles in swallowing (26). They examined twenty-one specimens. They found that muscle bundles from the palatopharyngeus and stylopharyngeus muscles were related to the tonsils in a way that when contracted, they move the tonsils laterally to permit and wide and unobstructed pharyngeal port (26). Interestingly, from the results of this study one might suggest that dysfunction in the palatopharyngeus and stylopharyngeus muscles might contribute to OSA refractory to tonsillectomy and

DocuSign Envelope ID: FF917FA4-BEA0-4E08-96D0-A9016C337F14

adenoidectomy in children, as the underlying cause could be due to the lack of muscle tone and not tonsil size in these patients.

Although large tonsils are the most common risk factor for OSA, a 2005 study by Arens et al. looked at the underlying anatomy and function of the upper airway in pediatric patients with OSA to determine if these were different than children without OSA (27). Using MRI, they measured dynamic airway change during the respiratory cycle in both groups. They found that children with OSA had significantly narrower upper airway dimensions than those without OSA, along with significantly greater fluctuation in airway size during respiration. It is important to note that almost all of the fluctuation occurred in the lateral direction, corresponding to the orientation of the stylopharyngeus muscle. They state that upper airway dimensions changed very little during respiration in normal children. (27, 53). Clearly, even though large tonsils may cause pediatric OSA, lack of muscle tonicity is an issue than must be considered. Patients with lack of muscle tone in the upper airway have a more difficult time maintaining a patent airway, which may be the underlying cause of the OSA, not large tonsils alone.

Studies have examined the possibility of having patients perform specific oropharyngeal exercises as a treatment modality for OSA. The

DocuSign Envelope ID: FF917FA4-BEA0-4E08-96D0-A9016C337F14

goal for these exercises is to increase to neuromuscular tone of the pharyngeal muscles, increasing the patient's ability to maintain a patent airway. A 2008 randomized controlled trial by Guimaraes et al. concluded that oropharyngeal exercises significantly reduce OSA severity and symptoms and represent a promising treatment modality for moderate OSA (29). A 2014 systematic review on the topic by Camacho et al. looked at nine adult studies and two pediatric studies and performed a meta-analysis to determine the effectiveness of myofunctional therapy as an OSA treatment. They concluded that myofunctional therapy decreases the apnea-hypopnea index by approximately 50% in adults and 62% in children (28). They suggested that myofunctional therapy can serve as a viable adjunct to other OSA therapies (28). In 2013, Guilleminault at al. looked at the role of myofunctional therapy as an adjunctive treatment to adenotonsillectomy (AT) in pediatric OSA in a non-randomized, retrospective case series. In 24 patients, 11 underwent myofunctional therapy following AT, while 13 did not. The study found that those who did not undergo myofunctional therapy saw a recurrence of SDB symptoms at long term follow up (AHI 5.3+-1.5), while those who underwent myofunctional therapy revealed a healthy AHI at the same time point (30). In 2016, Aiello et al looked at the effect of exercise

DocuSign Envelope ID: FF917FA4-BEA0-4E08-96D0-A9016C337F14

training in a systemic review and found that differences in AHI in OSA patients who participate in oropharyngeal exercise and those who do not is statistically significant. They argue that oropharyngeal exercise is the only current treatment modality available that directly address the cause of OSA, decreased neuromuscular tone of the upper airway (31). In all, it seems that oropharyngeal exercises can in fact increase the neuromuscular tone of pharyngeal muscles, allowing the patient to maintain a patent airway more easily. These studies also provide further evidence that decreased muscular tone and increased collapsibility of the airway are at the basis of obstructive sleep apnea.

Hard tissue anatomical characteristics can play a role in the development in obstructive sleep apnea, however, neuromuscular dysfunction and airway collapsibility are the primary causal factors. A study by Vos et al in 2010 looked at the static anatomical characteristics of the upper airway and determined that airway morphology alone is not enough to make an OSA diagnosis, but may help determine the ideal treatment for the patient (32). In the 2019 AAO white paper on Obstructive Sleep Apnea, Behrents et al. describe that craniofacial morphologies such as mandibular retrognathia, long and narrow faces, narrow and deep palate, low hyoid position, and midface deficiency may predispose the patient to OSA (5). They emphasize, however, that

DocuSign Envelope ID: FF917FA4-BEA0-4E08-96D0-A9016C337F14

the strength of relationship between these craniofacial morphologies and the development of OSA is not well established (5). An exception to this would be craniofacial anomalies such as Pierre Robin sequence and syndromic craniosynostosis, which carry a high prevalence of OSA (5). New imaging techniques such as cone-beam computed tomography (CBCT) allow for direct visualization of the hard tissues of the upper airway, but have major limitations in the diagnosis of OSA. Behrents et al. state that CBCT provides no information on neuromuscular tone, collapsibility, or actual function of the airway, and they argue that CBCT is not sufficient as a risk assessment tool for OSA (5). In sum, there are certain hard tissue characteristics that may predispose the individual to OSA, but the function and collapsibility of the upper airway are the ultimate causal factor in the development of obstructive sleep apnea.

Current Screening, Imaging and Diagnostic Techniques for OSA

The diagnostic gold standard for both pediatric and adult obstructive sleep apnea is polysomnography (PSG). PSG is a multichannel recording of sleep that typically occurs in a sleep laboratory (4). Because PSG diagnoses OSA in terms of airflow cessation or limitation, respiratory effort, oxygen desaturation, and sleep

DocuSign Envelope ID: FF917FA4-BEA0-4E08-96D0-A9016C337F14

disruption, PSG only indirectly describes collapse of the upper airway. PSG does not allow for direct visualization of the upper airway (4). PSG is also costly, time consuming, and invasive. Because of this, over the past fifteen years numerous studies have tried to better visualize the upper airway in the pediatric population to improve OSA diagnosis and personalize treatment (33). In a 2019 review of airway imaging, Quinlan et al. went on to describe all airway imaging modalities available at the time. They reviewed the literature on lateral cephalometry, cone beam computed tomography (CBCT), MRI, and drug induced sleep endoscopy. They found that lateral cephalometry was the least useful of all imaging techniques, as the patient is in an upright position and the image is in just 2 dimensions. CBCT is better as it offers a 3-dimensional image of the airway, however it is a static image and does not portray the function or dynamics of the airway (5). They found that MRI offers a good method to visualize the upper airway and soft tissue dynamically. However, they state that MRI is of limited value in children as they are noisy, have long acquisition times, and sometimes require the child to be sedated, which may not allow for an accurate estimate of airway collapse as muscles may be in a more relaxed state than usual (33). The final imaging modality described, drug induced sleep endoscopy (DISE), allows for direct visualization of the area of obstruction. A flexible

DocuSign Envelope ID: FF917FA4-BEA0-4E08-96D0-A9016C337F14

endoscope is inserted through the nose of a sedated child and positioned at different areas to visualization the exact area of obstruction. However, they argue that because the child is sedated, like MRI, the upper airway dynamics might not be representative as those during sleep (33). To conclude the review, the author's state that there is still not enough evidence for these imaging modalities to replace PSG for diagnosis of OSA, despite recent advances (33).

It is important to note that of all these methods described in the previous study, the only method capable of providing good definition of soft tissues is MRI. A 2014 descriptive study by Nayak and Fleck investigated the use of cine MRI for dynamic 2D imaging of the upper airway. Images are obtained over a 30 second or longer interval and then played back as a video, allowing for a clear image of upper airway dynamics (34). They advocate for the use of cine MRI to localize the area of airway obstruction to allow for more customized treatment.

Another area of some debate in the literature is the best way to screen for pediatric OSA in routine practice with questionnaires. In 2010, Spruyt and Gozal published a review of all current questionnaires used to screen for pediatric OSA in clinical practice. They identified 57 questionnaires, and of those only 2 questionnaires fulfilled all what they

DocuSign Envelope ID: FF917FA4-BEA0-4E08-96D0-A9016C337F14

termed as "desirable criteria" for proper screening of pediatric OSA screening. 11 other questionnaires fulfilled most of the "desirable criteria". They argue that too many questionnaires are being used that have not undergone careful validation processes (35). They advocate for careful examination of the pediatric screening tools used in clinical practice as some may lead to misinformation (35).

The pediatric sleep questionnaire (PSQ) is a validated tool to screen for children with obstructive sleep apnea. Positive answers to 33% or more (7 of 22) of the items on the pediatric sleep questionnaire is considered high risk (6). A 2020 study by Abtahi et al. used the PSQ to determine the presence of sleep-disordered in the orthodontic population. They reviewed 390 patient charts, and found that 10.8% of these patients were at high risk based on answers to the PSQ (6). This was greater than the previously reported 5% in the general population. A 2019 study by Pabary et al. further examined the efficacy of the PSQ by examining how well the PSQ predicts the presence of sleep apnea in children with underlying conditions such as trisomy 21 and various neuromuscular disorders. They found that in this subset of the pediatric population, the pediatric sleep questionnaire may miss the diagnosis of OSA in patients with underlying conditions. Thus, it is important to

DocuSign Envelope ID: FF917FA4-BEA0-4E08-96D0-A9016C337F14

carefully examine those with underlying conditions for OSA to ensure the diagnosis is not missed (36).

An interesting study published in 2017 by Gozal and Gozal reviewed the current evidence for the presence of morbidity-related biomarkers existing in children with OSA (37). They wanted to try and understand why some patients with the same PSG readings have much different symptoms of OSA. They were able to identify 8 current biomarkers, each with its own comorbidity. Two of the eight biomarkers were associated with predicting residual OSA after adenotonsillectomy (37). Much more research must be done before identifying biomarkers can become clinically feasible, but it is an interesting screening modality on the horizon.

Other novel methods of measuring airway collapse to screen and diagnose OSA are arising in the literature. A 2019 study by Cuadrado et al. measured changes in upper airway resistance from a standing to supine position using a flow interruption device (38). They equated this change in resistance to the amount of upper airway collapse. They found that this method was able to predict the presence of moderate and severe OSA with high specificity, but recommended its use combined with other screening tools such as the STOP-BANG

DocuSign Envelope ID: FF917FA4-BEA0-4E08-96D0-A9016C337F14

questionnaire to provide a more complete risk assessment (38). Another novel method of screening for OSA is to directly visualize the upper airway using submental ultrasound. Submental ultrasound as a screening modality will be discussed on its own in the next section of the literature review.

Submental Ultrasound as a method to screen for OSA

Submental ultrasound to screen for OSA, the subject of this study, is a novel modality to directly visualize and assess for upper airway collapse. The technique was first described in 2013 by Shu et al. The study used submental ultrasound to quantify the amount of airway collapse in the transverse dimension for patients without OSA and for those with mild-moderate and severe OSA (39). Prior to taking the ultrasound scan, each patient had undergone a PSG sleep study to accurately determine the presence and severity of OSA. The study consisted of 50 patients with severe OSA, 30 with mild-moderate OSA, and 25 without OSA, all confirmed with PSG (39). The technician scanned each patient with the ultrasound probe in the retropalatal and retroglossal regions. Each patient would breathe normally and then perform the Mueller maneuver (39). The Mueller maneuver is performed when the patient attempts a vigorous inhale with the nose and mouth closed. This creates

DocuSign Envelope ID: FF917FA4-BEA0-4E08-96D0-A9016C337F14

negative pressure in the lungs and induces airway collapse. Following the scan, the authors reviewed the ultrasound images with specific computer software. They located the airway with each maneuver and measured the width of the airway interface (39). They then calculated a percentage collapse of both the retropalatal and retroglossal regions by dividing the width at Mueller maneuver with the width at normal tidal breathing. After quantifying the amount of airway collapse, the authors compared the amount of collapse between those without OSA, those with mild-moderate OSA, and those with severe OSA. They found that airway collapse in the retropalatal region was especially well correlated to OSA severity, particularly with Mueller maneuver. Along with this, they concluded that submental ultrasound can accurately measure pharyngeal airspace and adjacent soft tissue and argue that it is a viable method to discriminate OSA severity (39). They suggest that ultrasound may be a promising tool for screening for severe OSA patients for early intervention. One limitation of the study is that a pharyngeal pressure monitor was not used, so it was difficult to discern how vigorous each patient inhaled with Mueller maneuver. It is possible that some patients inhaled more vigorously than others without knowing, and this may lead to greater collapse and skew the data (39). In all, the study

DocuSign Envelope ID: FF917FA4-BEA0-4E08-96D0-A9016C337F14

determines that submental ultrasound as a screening tool is on the horizon and certainly has promise as a future screening tool for OSA.

A 2019 study by Lee et al. also examined the ability to predict OSA with submental ultrasound, but they took it one step further. They developed a robotic arm to automatically rotate the ultrasound probe and try and remove human error from the procedure (40). The robotic arm and positioning device used was an earlier model of the exact one used at Case Western Orthodontics for SDB screening. They enrolled 51 patients with OSA and 13 healthy volunteers. Similar to Shu et al., each patient underwent an ultrasound scan at both tidal breathing and during the Mueller maneuver. This machine repeated each scan twice for a total of three scans under each condition per patient (40). Computer software would then automatically identify the transverse airway diameter in all images and determine the mean amount of airway collapse in each patient at four regions of the airway. Using this technique, the study concluded that using BMI and median dynamic change of pharyngeal diameter as indicators, machine-held submental ultrasound could be applied to identify patients with OSA of different severity with good accuracy (40). It is important to note that this study used BMI in conjunction with airway collapse to determine risk, and not collapse alone.

DocuSign Envelope ID: FF917FA4-BEA0-4E08-96D0-A9016C337F14

A 2006 study by Miller et al. looked at the ability of ultrasound to visualize airway structures in lambs (41). They concluded that ultrasound imaging provides a modality for uninterrupted analysis of airway structural properties under static resting and dynamic loading conditions. They suggest that ultrasonography provides a means to evaluate respiratory therapies in a dynamic way (41). Although less relevant than the previous two mentioned studies, this study supports the notion of the ability for ultrasound to accurately detect the airway and surrounding soft tissues.

In conclusion, submental ultrasound is a novel technique to evaluate the dynamics of the airway and visualize airway collapse in real time. Although current literature on the topic is limited, it appears that this is a viable screening tool.

Screening for and relevance of OSA in Orthodontics

Two studies have looked at prevalence of sleep disordered breathing in an orthodontic population. The first study, performed by Rohra et al., took place in the orthodontics clinic at Case Western Reserve University and used the Pediatric Sleep Questionnaire to assess prevalence (42). The charts of 303 healthy children were reviewed, and any PSQ with 33% or more positive responses was considered high risk.

DocuSign Envelope ID: FF917FA4-BEA0-4E08-96D0-A9016C337F14

7.3% of the 303 patients were found to be high risk. Thus, the authors suggest that approximately 7% of orthodontic patients may be at risk for some form of significant sleep disordered breathing (42). Another study in 2020 by Abtahi et al. used similar methodology to estimate prevalence - using the PSQ and reviewing 390 charts (6). They found a higher prevalence than Rohra et al. in 2018, estimating that 10.8% were at high risk on the PSQ (6). Past studies assessing the prevalence of SDB in the general population have been estimated at 5%, so both studies support the idea that the prevalence of SDB in patients seeking orthodontic care is higher than that of the general population. As so, the orthodontist should absolutely include screening for SDB in their clinical exam. If not, many cases of SDB may go undiagnosed, and the patient will have been done a disservice.

Because cone-beam computed tomography (CBCT) has become more and more commonplace in orthodontics, a number of studies have been published comparing airway volume on CBCT and various malocclusions. A 2020 study by Tseng evaluated 90 CBCT images and tried to determine if pharyngeal airway volume differed between different skeletal patterns (43). The study found that skeletal class II patients – when compared to skeletal class I and III patients – showed significantly smaller total pharyngeal airway volume, velo-, hypo-, and

DocuSign Envelope ID: FF917FA4-BEA0-4E08-96D0-A9016C337F14

oropharyngeal airway volumes, as well as smallest cross sectional area (43). A 2011 study by Hakan El and Palomo had similar findings. They looked at the CBCT images of 140 patients and found that skeletal class II patients had significantly smaller oropharyngeal airway volume than that of skeletal class I and class III patients (44). A study by Nath et al. also compared differences in airway volume and certain skeletal patterns and found a statistically significant difference in airway volumes for differing ANB angle, SNB angle, and Wits appraisal among males and females (45). These studies seem to support the idea that a relationship exists between total airway volume and skeletal classification.

Other studies have been published assessing the accuracy and reliability of CBCT as a method to measure the upper airway. A 2018 study by Zimmerman et al. studied the intra-examiner and inter-examiner reliability of the complete process of volumetric and cross-sectional area assessments of the upper airway on CBCT (46). Six examiners of various levels of experience used the Dolphin imaging program to individually measure the airway volume and cross-sectional area of 10 patients. They found that reliability improved with examiner experience but was generally low for the hypopharynx and nasopharynx regions. The oropharynx was the only region found to have excellent intra-examiner and inter-examiner reliability. They conclude

DocuSign Envelope ID: FF917FA4-BEA0-4E08-96D0-A9016C337F14

that further studies are required before CBCT can be advocated as a valid and reliable method for comparisons of upper airway dimensions between patients (46). A second study published in 2010 by Hakan and Palomo aimed to compare reliability and accuracy of three commercially available software for measuring upper airway volume. They found that in measuring upper airway volume, reliability was high for all three programs, but accuracy was poor (47). They argue that more work needs to be done before automatic airway segmentation can be accepted as a valid procedure. This study seems to coincide with the results of Zimmerman et al. 2018, showing that volume measurements of the upper airway in CBCT may not be accurate and thus may not be a valid way of imaging the upper airway.

A 2012 systematic review by Alsufyani et al. aimed to asses using CBCT to measure dimensional changes in the upper airway after appliance or surgical therapy in patients with OSA (48). Seven articles met their criteria and were included in the review. They found that there is insufficient literature pertaining to the use of CBCT to assess treatment outcomes to draw a conclusion. They state that more high-quality evidence level studies are needed to determine if CBCT airway dimensional changes are a valid measure of treatment outcome (48). To sum all these studies, it appears that although a relationship may exist

DocuSign Envelope ID: FF917FA4-BEA0-4E08-96D0-A9016C337F14

between skeletal classification and airway volume, CBCT is not accurate enough to be used as a screening or diagnostic tool for OSA. In the AJO-DO 2019 white paper on OSA, Behrents et al. support this statement, stating that CBCT does not provide a proper risk assessment technique or screening method for OSA as it does not account for neuromuscular tone, susceptibility of the airway to collapse, or function of the airway (5). They also state that there is no direct link between radiographic measures of airway size or shape and PSG results (5). It seems that CBCT is currently not an adequate method to screen for OSA, which is unfortunate because it is becoming more and more commonplace in orthodontic practice.

Last, this section of the literature review will touch on the role of the orthodontist in the treatment of OSA. A 2018 study by Galeotti et al evaluated the prevalence of malocclusion in children with OSA (49). They assessed canine relationship, presence of a posterior crossbite, overbite and overjet in 139 children with OSA and 137 healthy children. They found a high prevalence of malocclusion in children with OSA compared to the control group. Of the occlusal characteristics recorded, posterior crossbite and excessive overjet and overbite were significantly associated with OSA (49). According to Behrents et al. in the AJO-DO white paper, there is low level evidence that rapid maxillary

DocuSign Envelope ID: FF917FA4-BEA0-4E08-96D0-A9016C337F14

expansion and mandibular advancement devices decrease AHI in children. However, they emphasize that these appliances should only be used as a treatment modality for OSA in cases where an actual skeletal discrepancy and orthodontic indication exist (5).

In patients who cannot tolerate or are non-compliant with CPAP, mandibular advancement appliances may be prescribed by a sleep physician for the orthodontist's use. A 2020 study by Lai et al. assessed the effectiveness of oral appliances versus CPAP in patients with severe OSA and mandibular retrognathia (50). They found that CPAP and oral appliances are both effective in treating OSA when mandibular retrognathia is present. They found that mandibular advancement oral appliances are more effective in treating OSA patients with mandibular retrognathia than those without retrognathia. They also found that CPAP was overall superior to oral appliances in approving PSG scores, but that compliance was higher with oral appliances than with CPAP (50). The American Academy of Sleep Medicine (AAOSM) has recommended oral appliances for use in patients with primary snoring and mild-moderate OSA (51). In all, the oral appliances certainly have a place in OSA treatment. However, there is little literature on the use of oral appliance therapy for OSA treatment in children. If retrognathia is present in the child, it is better addressed with growth modification

DocuSign Envelope ID: FF917FA4-BEA0-4E08-96D0-A9016C337F14

through orthodontic treatment than with an OSA oral appliance, and is thus likely why there is not much evidence on the use of oral appliances in children.

To conclude, Lavigne et al. in 2019 provide a nice description of the role of the dentist/orthodontist in the management of OSA (52). This role includes screening patients for OSA risk factors, referring to the appropriate health professionals as indicated, and providing oral appliance therapy followed by regular dental and sleep medicine follow up (52).

DocuSign Envelope ID: FF917FA4-BEA0-4E08-96D0-A9016C337F14

LITERATURE REVIEW REFERENCES

1. Kryger MH. Diagnosis and management of sleep apnea syndrome. *Clinical Cornerstone*. 2000; 2(5): 39-44.

2. Semelka M, Wilson J, Floyd R. Diagnosis and Treatment of Obstructive Sleep Apnea in Adults. *American Family Physician*. 2016; 94(5): 355-360.

3. D'Agostino MA. Obstructive sleep apnea, diagnosis, management, and treatment. *Otolaryngologic Clinics of North America*. 2016; 49(6): xiii-xiv.

4. Yu JL, Afolabi-Brown O. Updates on management of pediatric obstructive sleep apnea. *Pediatric Investigation*. 2019; 3(4): 228-235.

5. Behrents RG, Shelgikar AV, Conley RS, Flores-Mir C, Hans MG, Levine M, Palomo JM, Hittner J. Obstructive sleep apnea and orthodontics: An American Association of Orthodontists white paper. *American Journal of Orthodontics and Dentofacial Orthopedics*. 2019; 156(1): 13-28.

6. Abtahi S, Witmans M, Alsufyani NA, Major MP, Major PW. Pediatric sleep-disordered breathing in the orthodontic population: Prevalence of positive risk and associations. *American Journal of Orthodontics and Dentofacial Orthopedics*. 2020; 157(4).

7. Lumeng JC, Chervin RD. Epidemiology of pediatric obstructive sleep apnea. *Proceedings of the American Thoracic Society*. 2008; 5(2): 242-252.

8. Guilleminault C, Korohkin R, Winkle R. A review of 50 children with obstructive sleep apnea syndrome. *Lung*. 1981; 159: 275-287.

9. Gipson K, Lu M, Kinane TB. Sleep-disordered breathing in children. *Pediatrics in Review*. 2019; 40(1): 3-13.

10. Huang Y, Guilleminault C. Pediatric obstructive sleep apnea: Where do we stand? *Sleep-Related Breathing Disorders*. 2017; 136-144.

DocuSign Envelope ID: FF917FA4-BEA0-4E08-96D0-A9016C337F14

11. Savini S, Ciorba A, Bianchini C, Stomeo F, Corazzi V, Vicini C, Pelucchi S. Assessment of obstructive sleep apnea (osa) in children: An update. *Acta Otorhinolaryngologica Italica*. 2019; 39(5): 289-297.

12. Gozal D, Burnside MM. Increased upper airway collapsibility in children with obstructive sleep apnea during wakefulness. *American Journal of Respiratory and Critical Care Medicine*. 2004; 169(2): 163-167.

13. Lo Bue A, Salvaggio A, Insalaco G. Obstructive sleep apnea in developmental age. a narrative review. *European Journal of Pediatrics*. 2020; 179(3): 357-365.

14. Chandrakantan A, Musso MF, Floyd T, Adler AC. Pediatric obstructive sleep apnea: Preoperative and neurocognitive considerations for perioperative management. *Pediatric Anesthesia*. 2020; 30(5): 529-536.

15. Greig SR. Current perspectives on the role of tonsillectomy. *Journal of Paediatrics and Child Health*. 2017; 53(11): 1065-1070.

16. Marcus CL, Moore RH, Rosen CL, Giordani B, Garetz SL, Taylor HG, Redline S. A randomized trial of adenotonsillectomy for childhood sleep apnea. *New England Journal of Medicine*. 2013; 368(25): 2366-2376.

17. Venekamp, Roderick P. Tonsillectomy or Adenotonsillectomy versus Non-Surgical Management for Obstructive Sleep-Disordered Breathing in Children. *Cochrane Database of Systematic Reviews*. 2015.

18. Rana M, August J, Levi J, Parsi G, Motro M, DeBassio W. Alternative approaches to Adenotonsillectomy and continuous positive airway pressure (CPAP) for the management of Pediatric obstructive sleep Apnea (osa): A review. *Sleep Disorders*. 2020; 1-11.

DocuSign Envelope ID: FF917FA4-BEA0-4E08-96D0-A9016C337F14

19. Ehsan Z, Ishman SL. Pediatric obstructive sleep apnea. *Otolaryngologic Clinics of North America*. 2016; 49(6): 1449-1464.

20. Choi D, Bae J, Hu K, Kim H. Anatomical variations of the stylopharyngeus and superior constrictors in relation to their function. *Anatomy & Cell Biology*. 2020; 53(4): 417-421.

21. Fukino K, Tsutsumi M, Sanudo J, Ono T, Akita K. Anatomical significance of the spatial distribution of the palatopharyngeus with regard to velopharyngeal closure. *The Cleft Palate-Craniofacial Journal*. 2018; 56(6): 744-750.

22. Sakamoto Y. Classification of pharyngeal muscles based on innervations from glossopharyngeal and vagus nerves in human. *Surgical and Radiologic Anatomy*. 2009; 31(10): 755-761.

23. Guilleminault C, Hill MW, Simmons F, Dement WC. Obstructive sleep apnea: Electromyographic and fiberoptic studies. *Experimental Neurology*. 1978; 62(1): 48-67.

24. Mitchinson AG, Yoffey JM. Respiratory Displacement of Larynx, Hyoid Bone and Tongue. *Journal of Anatomy*. 1947; 81(1): 118-122.

25. Tong J, Jugé L, Burke PG, Knapman F, Eckert DJ, Bilston LE, Amatoury J. Respiratory-related displacement of the trachea in obstructive sleep apnea. *Journal of Applied Physiology*. 2019; 127(5): 1307-1316.

26. Rood SR, Langdon H, Klueber K, Greenberg E. Muscular anatomy of The Tonsil And Tonsillar bed: A reexamination. *Otolaryngology–Head and Neck Surgery*. 1979; 87(4): 401-408.

27. Arens R, Sin S, McDonough JM, Palmer JM, Dominguez T, Meyer, H, Pack AI. Changes in upper airway size during tidal breathing in children with obstructive sleep apnea syndrome. *American Journal of Respiratory and Critical Care Medicine*. 2005; 171(11): 1298-1304.

28. Camacho M, Certal V, Abdullatif J, Zaghi S, Ruoff CM, Capasso R, Kushida CA. Myofunctional therapy to treat obstructive sleep

DocuSign Envelope ID: FF917FA4-BEA0-4E08-96D0-A9016C337F14

Apnea: A systematic review and meta-analysis. *Sleep*. 2015; 38(5): 669-675.

29. Guimarães KC, Drager LF, Genta PR, Marcondes BF, Lorenzi-Filho, G. Effects of oropharyngeal exercises on patients with moderate obstructive sleep apnea syndrome. *American Journal of Respiratory and Critical Care Medicine*. 2009; 179(10): 962-966.

30. Guilleminault C, Huang Y, Monteyrol P, Sato R, Quo S, Lin C. Critical role of myofascial reeducation in pediatric sleep-disordered breathing. *Sleep Medicine*. 2013; 14(6): 518-525.

31. Aiello KD, Caughey WG, Nelluri B, Sharma A, Mookadam F, Mookadam M. Effect of exercise training on sleep apnea: A systematic review and meta-analysis. *Respiratory Medicine*. 2016; 116: 85-92.

32. Vos WG, De Backer WA, Verhulst, SL. Correlation between the severity of sleep apnea and upper airway morphology in pediatric and adult patients. *Current Opinion in Allergy & Clinical Immunology*. 2010; 10(1): 26-33.

33. Quinlan CM, Otero H, Tapia IE. Upper airway visualization in pediatric obstructive sleep apnea. *Paediatric Respiratory Reviews*. 2019; 32: 48-54.

34. Nayak KS, Fleck RJ. Seeing sleep: Dynamic imaging of upper airway collapse and collapsibility in children. *IEEE Pulse*. 2014; 5(5): 40-44.

35. Spruyt K, Gozal D. Pediatric sleep questionnaires as diagnostic or epidemiological tools: A review of currently available instruments. *Sleep Medicine Reviews*. 2011; 15(1): 19-32.

36. Pabary R, Goubau C, Russo K, Laverty A, Abel F, Samuels M. Screening for sleep-disordered breathing with pediatric sleep questionnaire in children with underlying conditions. *Journal of Sleep Research*. 2019; 28(5).

37. Kheirandish-Gozal L, Gozal D. Pediatric osa syndrome morbidity biomarkers. *Chest*. 2017; 151(2): 500-506.

DocuSign Envelope ID: FF917FA4-BEA0-4E08-96D0-A9016C337F14

38. Cuadrado GR, Álvarez RF, Huertas JH, Lopez MJ, Urrutia MI, Clara PC. Measurement of upper airway resistances: A simple way to assess its collapsibility? *Sleep and Breathing*. 2020; 24(4): 1531-1535.

39. Shu C, Lee P, Lin J, Huang C, Chang Y, Yu C, Wang H. The use of sub-mental ultrasonography for identifying patients with severe obstructive sleep apnea. *PLoS ONE*. 2013; 8(5).

40. Lee P, Shu C, Kuo Y, Chen C, Wang H, Chen A, Chia-Hao Liu E. An effective mode to predict severity of obstructive sleep apnea: Dynamic change of aerospace detected by submental ultrasonography. *Sleep*. 2019; 42(Supplement 1).

41. Miller TL, Altman AR, Tsuda T, Shaffer TH. An ultrasound imaging method for in vivo tracheal bulk and Young's moduli of elasticity. *Journal of Biomechanics*. 2007; 40(7): 1615-1621.

42. Rohra AK, Demko CA, Hans MG, Rosen C, Palomo JM. Sleep disordered breathing in children seeking orthodontic care. *American Journal of Orthodontics and Dentofacial Orthopedics*. 2018; 154(1): 65-71.

43. Tseng Y, Tsai F, Chou S, Hsu C, Cheng J, Chen C. Evaluation of pharyngeal airway volume for different dentofacial skeletal patterns using cone-beam computed tomography. *Journal of Dental Sciences*. 2021; 16(1): 51-57.

44. El H, Palomo JM. Airway volume for different dentofacial skeletal patterns. *American Journal of Orthodontics and Dentofacial Orthopedics*. 2011; 139(6).

45. Nath M, Ahmed J, Ongole R, Denny C, Shenoy N. CBCT analysis of pharyngeal Airway volume and comparison of Airway volume among patients with skeletal Class I, Class II, and Class III malocclusion: A retrospective study. *CRANIO®*. 2019; 1-12.

DocuSign Envelope ID: FF917FA4-BEA0-4E08-96D0-A9016C337F14

46. Zimmerman JN, Vora SR, Pliska BT. Reliability of upper airway assessment using CBCT. *European Journal of Orthodontics*. 2018; 41(1): 101-108.

47. El H, Palomo JM. Measuring the airway in 3 dimensions: A reliability and accuracy study. *American Journal of Orthodontics and Dentofacial Orthopedics*. 2010; 137(4).

48. Alsufyani NA, Al-Saleh MA, Major PW. CBCT assessment of upper airway changes and treatment outcomes of obstructive sleep apnea: A systematic review. *Sleep and Breathing*. 2013; 17(3): 911-923.

49. Galeotti A, Festa P, Viarani V, D'Antò V, Sitzia E, Piga S, Pavone M. Prevalence of malocclusion in children with obstructive sleep apnea. *Orthodontics & Craniofacial Research*. 2018; 21(4): 242-247.

50. Lai H, Huang W, Chen W, Wang D. Effectiveness of continuous positive airway pressure versus mandibular advancement device in severe obstructive sleep Apnea patients with mandibular retrognathia: A prospective clinical trial. *Ear, Nose & Throat Journal*. 2020.

51. Padma A, Ramakrishnan N, Narayanan V. Management of obstructive sleep apnea: A dental perspective. *Indian Journal of Dental Research*. 2007; 18(4): 201.

52. Lavigne G, Herrero-Babiloni A, Beetz G, Dal-Fabbro C, Sutherland K, Huynh N, Cistulli P. Critical issues in dental and medical management of obstructive sleep apnea. *Journal of Dental Research*. 2019; 99(1): 26-35.

53. Dewald D. Pharyngeal anatomy. University Hospitals, 28 May 2021, Cleveland, Ohio. Lecture.

DocuSign Envelope ID: FF917FA4-BEA0-4E08-96D0-A9016C337F14

STATEMENT OF THESIS

The purpose of this study was to use submental ultrasound data to examine the amount and pattern of airway collapse observed in pediatric orthodontic patients with varying degrees of signs and symptoms of sleep disordered breathing (SDB).

The amount and pattern of airway collapse will be compared among subjects, as well as between subjects and adults with and without OSA.

DocuSign Envelope ID: FF917FA4-BEA0-4E08-96D0-A9016C337F14

MANUSCRIPT FOR PUBLICATION

DocuSign Envelope ID: FF917FA4-BEA0-4E08-96D0-A9016C337F14

COMPARISON OF AIRWAY COLLAPSIBILITY IN CHILDREN WITH SIGNS AND SYMPTOMS OF SLEEP DISORDERED BREATHING USING SUBMENTAL ULTRASOUND

Authors: Craig Madison D.M.D.[1]

Juan Martin Palomo D.D.S., M.S.D.[2]

Denise Dewald M.D.[3]

Mark Hans, D.D.S., M.S.D.[4,5]

1. Resident, Department of Orthodontics, Case Western Reserve University, Cleveland, OH, USA

2. Professor and Program Director, Department of Orthodontics, Case Western Reserve University, Cleveland, OH, USA

3. Sleep Research Fellow, Department of Sleep Medicine, University Hospitals, Cleveland, OH, USA

4. Professor and Department Chair, Department of Orthodontics, Case Western Reserve University, Cleveland, OH, USA

5. Private Practice in Orthodontics, Berea, OH, USA

Corresponding author:

Craig Madison

Case Western Reserve University

School of Dental Medicine

Department of Orthodontics

9601 Chester Avenue

Cleveland, OH, 44106

CJM253@case.edu

DocuSign Envelope ID: FF917FA4-BEA0-4E08-96D0-A9016C337F14

Introduction

Sleep-disordered breathing (SDB) encompasses a subset of conditions ranging from snoring, to upper airway resistance syndrome, to obstructive sleep apnea[1]. Of the conditions on the SDB spectrum, habitual snoring and obstructive sleep apnea (OSA) are the most common, with OSA representing the most severe manifestation[1]. OSA is characterized by obstruction of the upper airway during sleep. This airway obstruction – the result of narrowing or "collapse" of the upper respiratory passages – leads to a decrease or complete cessation of breathing (hypopnea or apnea, respectively)[2,3]. These breathing disruptions lead to repeated arousals that affect sleep continuity, thus depriving the individual of deep, restful sleep[3]. Expectedly, this leads to chronic fatigue and daytime sleepiness. Other conditions, such as hypertension, congestive heart failure, cardiac arrhythmias, and depression are associated with obstructive sleep apnea[3,4]. SDB and OSA affect patients of all ages. Studies have estimated pediatric SDB prevalence at 5% in the general population and estimated those at high risk for SDB at 7-10% in the orthodontic population[1,5,6]. Pediatric OSA has a different clinical presentation than that of adults. In contrast to adults – where the cardinal symptom of OSA is excessive daytime sleepiness – pediatric OSA is characterized less by daytime sleepiness and more by

DocuSign Envelope ID: FF917FA4-BEA0-4E08-96D0-A9016C337F14

disturbed nocturnal sleep[7]. This disturbed sleep negatively affects the pediatric patient's neurocognitive development, which leads to behavioral problems, struggles in school, hyperactivity, depression, insomnia, and psychiatric problems[8]. Beyond the mental health effects of SDB in the child, disrupted sleep can be a major psychological stressor for children and their families[7,9]. Early diagnosis of pediatric OSA may reduce the occurrence of neurocognitive and systemic complications over time, although diagnosis is often made too late due to under-recognition by practitioners[10]. As so, adequate screening and diagnosis of SDB and OSA in the pediatric population is of the utmost importance.

The underlying etiology of both adult and pediatric OSA is complex, and although adult and pediatric OSA have similar etiologic factors, there are some differences. For example, lymphoid hyperplasia and growth-related changes of the upper airway contribute to the presence and resolution of pediatric OSA, respectively. This is clearly not seen in adult OSA, as these patients have completed growth[11-13]. However, in both adult and pediatric OSA, impaired neuromuscular tone underlies the upper airway collapse seen in pediatric OSA. Studies have shown that during sleep, patients with obstructive sleep apnea showed a significant or complete disappearance of electromyogram activity in the pharyngeal muscles, including the stylopharyngeus

DocuSign Envelope ID: FF917FA4-BEA0-4E08-96D0-A9016C337F14

muscle[14]. The stylopharyngeus is very important in maintaining airway patency in the transverse dimension, as its contraction pulls the airway in a superior and lateral dimension bilaterally. Decreased activity of this muscle would result in an airway more susceptible to lateral collapse in the transverse plane of space[14-16]. A study by Arens et al. found that children with OSA had significantly narrower upper airway dimensions than those without OSA, along with significantly greater fluctuation in airway size during respiration. It is important to note that almost all of the fluctuation occurred in the lateral direction, corresponding to the orientation of the stylopharyngeus muscle[16-18]. Clearly, collapsibility of the airway plays a role in both adult and pediatric SDB.

At present, the diagnostic gold standard of OSA is overnight polysomnography (PSG), commonly referred to as a "sleep study". PSG is a multichannel recording of sleep that typically occurs in a sleep laboratory[19]. PSG diagnoses OSA in terms of airflow cessation or limitations, respiratory effort, oxygen desaturation, and sleep disruptions. While this is the gold standard, PSG only indirectly describes collapse of the upper airway. It does not allow for direct visualization of the airway dynamics underlying OSA[19]. Because of this, numerous studies over the last fifteen years have tried to better visualize the upper airway in both the adult and pediatric population to improve OSA diagnosis and

DocuSign Envelope ID: FF917FA4-BEA0-4E08-96D0-A9016C337F14

personalize treatment[20]. Until recently, the only methods for imaging the airway dynamically were with MRI and drug-induced sleep endoscopy (DISE). MRI is noisy, has long acquisition times, and sometimes requires the child to be sedated, which may not allow for an accurate estimate of airway collapse as muscles may be in a more relaxed state than usual. DISE requires the patient to be sedated, and incurs the risks inherent with general anesthesia[20,21].

Submental ultrasound as a method to screen for OSA is a novel imaging modality to visualize and assess for lateral upper airway collapse. Submental ultrasound (US) is a radiation free, non-invasive, and time efficient imaging modality. The technique was first described in 2013 by Shu et al., when they used submental ultrasound to quantify the amount of lateral airway collapse for patients without OSA and for those with mild-moderate and severe OSA[22]. Prior to taking the ultrasound scan, each patient had undergone a sleep study to accurately determine the presence and severity of OSA. The technician scanned each patient with the ultrasound probe to visualize the airway at the level of the soft palate and tongue base. Each patient would breathe normally and then perform the Muller maneuver[22]. The Muller maneuver is performed when the patient attempts a vigorous inhale with the nose and mouth closed. This creates negative pressure in the

DocuSign Envelope ID: FF917FA4-BEA0-4E08-96D0-A9016C337F14

lungs and induces airway collapse. They then calculated the percentage lateral collapse of the airway between normal breathing and Muller maneuver. They concluded that submental ultrasound can accurately measure pharyngeal airspace and adjacent soft tissue and argue that it is a viable method to discriminate OSA severity[22]. They suggested that ultrasound may be a promising tool for screening for severe OSA patients for early intervention. As so, it seems submental ultrasound provides the first way to visualize collapsibility of the airway in real-time in a non-invasive, radiation-free way in the office setting. The ultrasound scan data reviewed in this study was originally obtained in a similar method as Shu et al., except that the ultrasound unit used at CWRU Department of Orthodontics uses a machine arm to hold the probe and laser patient positioning to minimize error.

To our knowledge, this is the first study of its kind to look at lateral collapse of the airway in pediatric orthodontic patients. We believe that this study will provide some valuable insight into the nature of collapse of the upper airway in pediatric patients at risk for sleep disordered breathing, and will spur further research in this area.

DocuSign Envelope ID: FF917FA4-BEA0-4E08-96D0-A9016C337F14

Objectives

The purpose of this study was to use submental ultrasound data to examine the amount and pattern of lateral airway collapse observed in children with varying degrees of signs and symptoms of sleep disordered breathing (SDB). The amount and pattern of airway collapse was compared amongst subjects, as well as between subjects and adults with and without OSA.

DocuSign Envelope ID: FF917FA4-BEA0-4E08-96D0-A9016C337F14

Materials and Methods

This retrospective, descriptive study was approved by the Case Western Reserve University (CWRU) Institutional Review Board (IRB) (Appendix A). The inclusion criteria for the study were as follows: (1) patient of record at Case Western Reserve University, Department of Orthodontics, Core Clinic, (2) age 11-17, (3) patient must show signs and symptoms of sleep disordered breathing based on answers to the Pediatric Sleep Questionnaire or medical history, (4) patient must have had submental ultrasound taken as part of orthodontic records (to screen further for SDB). Exclusion criteria were as follows: (1) not a patient of record at Case Western Reserve University, Department of Orthodontics, Core Clinic, (2) outside the age range of 11-17, (3) no signs or symptoms of sleep disordered breathing, (4) no submental ultrasound taken as part of orthodontic screening or records, (5) patient has oral appliance in place that affects tongue posture or mandibular position.

303 patient charts were reviewed from the CWRU Department of Orthodontics, Core Clinic patient pool. For each subject, the Pediatric Sleep Questionnaire (PSQ) was reviewed to determine the subject's level of risk for, and symptoms of, sleep disordered breathing. The subject's medical and dental record was reviewed to assess for

DocuSign Envelope ID: FF917FA4-BEA0-4E08-96D0-A9016C337F14

craniofacial anomalies, diagnosis of neuromuscular disorder, or past orthodontic treatment/diagnoses. The subject's chart was further examined to determine whether a submental ultrasound was taken as part of orthodontic records to further assess risk of SDB. If the subject had both signs and symptoms of sleep disordered breathing and had an ultrasound scan taken, with no exclusion criteria, they were included in the study. Data collected included age, gender, height, weight, BMI, number of positive answers on the PSQ, whether or not "snoring more than half the time" was reported on the PSQ, whether or not the subject had a history of adenotonsillectomy, and the lateral airway collapse data from the ultrasound unit. The amount and pattern of lateral airway collapse was compared from subject to subject based on varying degrees of signs and symptoms of SDB. The data was further compared to the airway collapse ranges reported in Shu et al. 2013's study that gave airway collapse ranges for adult patients with confirmed mild/moderate and severe OSA, as well as without OSA.

Am-CAD UO Unit Background

In late 2020, CWRU School of Dental Medicine, Department of Orthodontics obtained an Am-Cad UO submental ultrasound unit to screen both adult and pediatric patients for OSA (Figure 1). Currently,

DocuSign Envelope ID: FF917FA4-BEA0-4E08-96D0-A9016C337F14

patients at risk for sleep disordered breathing and obstructive sleep apnea – as determined through clinical examination and screening questionnaires – undergo a submental ultrasound scan to further assess and quantify risk. Currently, all scans are performed by a single, trained operator.

To undergo a scan, the patient lies supine on an exam table with their head positioned in the headrest of the machine (Figure 2). The patient is positioned by adjusting the headrest until the laser guided positioner aligns with the hyoid-meatus plane, and then the probe is positioned on this same plane. Once the probe is positioned correctly, the resulting image is shown in figure 3, with the bright white line representing the width of the airway. When the scan is initiated, the probe rotates via a robotic arm to image the length of the upper airway. The patient breathes normally for the first scan and then performs the Muller maneuver for the second scan. To perform the Muller maneuver, the patient closes the nose and mouth and forcefully inhales, inducing airway collapse. The patient holds their breath after the forced inhale for the duration of the scan (approximately 6 seconds). Each scan is immediately repeated two more times. The computer software on the Am-CAD UO ultrasound tablet (Figure 4), automatically locates the airway interface in each scan. A depiction of the airway regions imaged

DocuSign Envelope ID: FF917FA4-BEA0-4E08-96D0-A9016C337F14

is shown in figure 5. Figure 6 shows the actual ultrasound images and airspace rendering. The yellow box is the area of interest indicating the proximity to the soft tissue-air interface, and the red area represents specifically what the software identifies as the anterior wall. The blue line is what the software measures as airspace width, depicted longitudinally across the airway regions. The normal breathing situation is depicted on the left side of the figure, and the Muller maneuver on the right side. The software then calculates the percentage shortening of this airway width at four regions of the airway – velum, oropharynx, tongue base, and epiglottis – between normal breathing and Muller maneuver. The percentage shortening of the width of the airway with the Muller maneuver corresponds to the amount of lateral collapse of the airway at the given region. To illustrate, looking back at figure 6 we see a subject with 31.84% shortening of the airway width – and thus – 31.84% lateral airway collapse at the tongue base between normal breathing and Muller maneuver. As so, each scan results in a percentage amount of lateral airway collapse at the velum, oropharynx, tongue base, and epiglottis. The entire scan process takes less than 10 minutes, and the patient can be immediately notified of OSA risk when present.

DocuSign Envelope ID: FF917FA4-BEA0-4E08-96D0-A9016C337F14

Results

Of the 303 patient charts reviewed, 18 met the inclusion criteria. The sample consisted of 10 males and 8 females, with an average age of 14.8 years. For each subject, the amount of lateral airway collapse was recorded at the velum, oropharynx, tongue base, and epiglottis, shown in Table I. Mean lateral airway collapse was calculated as velum 9.0% ± 9.6%, oropharynx 13% ± 10%, tongue base 16% ± 15%, and epiglottis 11% ± 8.0%, these results are shown in Table II. A graphical depiction of the amount and variation of lateral airway collapse for each subject is displayed in Figures 7 and 8. There was a wide amount of variation in the amount of lateral airway collapse across the sample, as shown by the large standard deviation in each category. 12 subjects showed at least 20% lateral airway collapse at some region of the airway, 8 subjects showed at least 30% lateral airway collapse at some region of the airway, and one subject showed almost 50% lateral airway collapse at one region in the airway. The remaining subjects had no greater than 20% lateral airway collapse. US3 showed very little lateral airway collapse, with no greater than 4% collapse at any region of the airway.

DocuSign Envelope ID: FF917FA4-BEA0-4E08-96D0-A9016C337F14

Lateral airway collapse was not uniform across the upper airway, with different amounts of collapse at different regions of the airway for each subject. This variation in the pattern of collapse was evident across the entire sample. For example, US1 had 36% lateral airway collapse at the velum, and very little collapse at the other three areas of the upper airway. US13 had 32% collapse at the tongue base, 18% at the epiglottis, but much less at the velum and oropharynx regions. Each subject had a unique pattern and amount of lateral airway collapse.

As part of the subject's orthodontic screening, four subjects had scans repeated to confirm their risk assessment, which allows for some insight into the repeatability of the ultrasound scans and machine. The amount of lateral airway collapse recorded with each repeated scan is shown in figure 9. Total amount of collapse was similar for US5, US7, and US11's repeated scans, but it was not similar for US17's scans. Further, the location of the airway implicated in greatest collapse (velum, oropharynx, tongue base, and epiglottis) was not the same for any of the repeated scans. It is possible that slight differences in patient positioning for the first and second scans led to the probe detecting the same area of the airway as different regions across both scans. Further investigations need to be done to determine the cause of the suboptimal repeatability, and whether it can be reduced by

DocuSign Envelope ID: FF917FA4-BEA0-4E08-96D0-A9016C337F14

standardization of tongue position, Muller maneuver, or enhanced attention to positioning (such as ensuring use of the same neck support in each session).

The patients at high risk for SDB according to the number positive answers on the Pediatric Sleep Questionnaire did not necessarily have the highest amounts of lateral airway collapse. US5 carried the second highest PSQ risk of the entire sample, but had no greater than 17% lateral airway collapse anywhere in the upper airway.

The mean amounts of lateral airway collapse found in this sample were considerably less than that of patients even without OSA in Shu et al's 2013 study using submental ultrasound in adult patients. For the sake of comparison, the velum and oropharynx were considered "retropalatal" regions, and tongue base and epiglottis considered "retroglossal" regions. An illustration of these regions of the airway and how they correspond to each other is shown in figure 10. Overall, both samples had large standard deviations highlighting a large variation in amounts of airspace collapse. The comparison is illustrated in table II.

DocuSign Envelope ID: FF917FA4-BEA0-4E08-96D0-A9016C337F14

Discussion

Submental ultrasound is a novel imaging technique that allows for dynamic imaging of the upper airway in a non-invasive, radiation free, accessible, and time efficient way. The purpose of this study was to use submental ultrasound data to examine the amount and pattern of lateral airway collapse observed in pediatric orthodontic patients with varying degrees of signs and symptoms of sleep disordered breathing (SDB). To the best of our knowledge, this is the first study of its kind.

This study found that lateral airway collapse was not uniform across the upper airway and that the amount and pattern of lateral airway collapse varied from subject to subject. One explanation for such variation could be due to individual variation in pharyngeal musculature. A study by Choi et al. looked at the distribution of pharyngeal musculature in dissected cadavers, and found that both the superior constrictor and stylopharyngeus muscles had multiple anatomical variants[15]. The stylopharyngeus muscle is the primary muscle responsible for maintaining the transverse dimension of the airway, and thus its function is indirectly measured with the amount of lateral airway collapse seen on submental ultrasound. It is possible that the different muscle fiber insertion patterns of stylopharyngeus as described by Choi

DocuSign Envelope ID: FF917FA4-BEA0-4E08-96D0-A9016C337F14

et al provide an explanation for the wide variation in contraction patterns amongst subjects.

Another possible explanation for the wide variation in the magnitude of contraction could be due to difficulty in standardizing the Muller maneuver. This is a limitation of submental ultrasound, as it is not possible to accurately determine how vigorously the patient is performing the Muller maneuver. It is possible that some patients inherently performed the maneuver more weakly than others, and this could have contributed to the wide variation in the magnitude of collapse. This may have also contributed to the questionable repeatability observed with the scans. We observed lower mean collapse values in our adolescent sample, compared with those reported in adults by Shu et al. 2013. This may have been related to the relatively shorter pharyngeal airway length in children as well as that facial growth is not yet completed in children compared to adults[23,24].

The level of risk prescribed by the Pediatric Sleep Questionnaire and the amount of lateral airway collapse observed on the ultrasound scans did not correlate in this small pilot sample. Those with highest PSQ risk did not necessarily show the highest amounts of lateral airway collapse. It is possible that the PSQ risk came from other factors, such as

DocuSign Envelope ID: FF917FA4-BEA0-4E08-96D0-A9016C337F14

nasal airway obstruction, large tonsils, or neurocognitive disorder. However, having both PSQ and lateral airway collapse values may help to provide a more comprehensive risk assessment for each patient with signs and symptoms of SDB. Knowing that airway collapse may not be the culprit of the SDB symptoms can help guide treatment decisions after a definitive diagnosis is reached by a sleep physician. This may be especially relevant to the field of orthodontics, as orthodontists are in a prime position to screen for SDB and even help treat the condition through oral appliances, rapid maxillary expansion, and mandibular advancement appliances in children. Orthodontic intervention as treatment for sleep apnea should only take place when an actual orthodontic indication exists, but having a more comprehensive risk profile could potentially help give the orthodontist an idea of the area that needs to be addressed and perform more customized treatment.

DocuSign Envelope ID: FF917FA4-BEA0-4E08-96D0-A9016C337F14

Conclusion

Submental ultrasound provides a way to dynamically image the airway in a non-invasive, radiation-free way. This study found that lateral airway collapse is not uniform across the upper airway. The amount and pattern of lateral airway collapse varied among each subject, with areas of greatest collapse often different amongst subjects. High risk on the Pediatric Sleep Questionnaire did not necessarily correlate with high lateral collapse of the airway. Repeatability of results over multiple scans was suboptimal, with significant irreproducibility of results across airway regions. Further investigations must be performed to clarify this finding.

DocuSign Envelope ID: FF917FA4-BEA0-4E08-96D0-A9016C337F14

Table I: Lateral Airway Collapse at Velum, Oropharynx, Tongue Base, and Epiglottis by Subject

Patient Number	Velum	Oropharynx	Tongue Base	Epiglottis
US 1	37%	0.0%	2.0%	5.2%
US 2	7.9%	16%	48%	0.0%
US 3	3.5%	0.0%	1.7%	3.6%
US 4	2.4%	14%	21%	16%
US 5	12%	16%	3.6%	14%
US 6	7.8%	7.3%	29%	5.3%
US 7	21%	33%	18%	12%
US 8	0.0%	30%	13%	12%
US 9	2.0%	0.0%	31%	15%
US 10	7.6%	23%	29%	12%
US 11	0.3%	12%	5.3%	1.6%
US 12	4.4%	14%	6.1%	12%
US 13	2.2%	9.0%	32%	18%
US 14	22%	33%	0.0%	7.9%
US 15	0.0%	8.1%	30%	25%
US 16	4.2%	6.3%	24%	28%
US 17	15%	9.1%	0.0%	15%
US 18	12%	8.3%	1.1%	0.0%

DocuSign Envelope ID: FF917FA4-BEA0-4E08-96D0-A9016C337F14

Table II: Comparison of airway contraction (collapse) values in this study (top) to that of Shu et al. 2013. (bottom)Velum and Oropharynx were compared to Retropalatal contraction (collapse), while Tongue Base and Epiglottis were compared to Retroglossal contraction (collapse). Mean values in this study were considerably less than even patients without OSA in Shu et al 2013.

Airspace Width Contraction (%) Current Study	
Velum	9.0 ± 9.6
Oropharynx	13 ± 10
Tongue Base	16 ± 15
Epiglottis	11 ± 8.0

Airspace Width Contraction (%) Shu et al. 2013			
	No OSA	Mild/Moderate OSA	Severe OSA
Retropalatal	21 ± 8.1	35 ± 9.3	50 ± 20
Retroglossal	25 ± 8.9	28 ± 7.5	34 ± 17

DocuSign Envelope ID: FF917FA4-BEA0-4E08-96D0-A9016C337F14

Figure 1: The AmCAD-UO ultrasound system with patient (left), and a labeled diagram of the of the AmCAD-UO ultrasound unit (right)

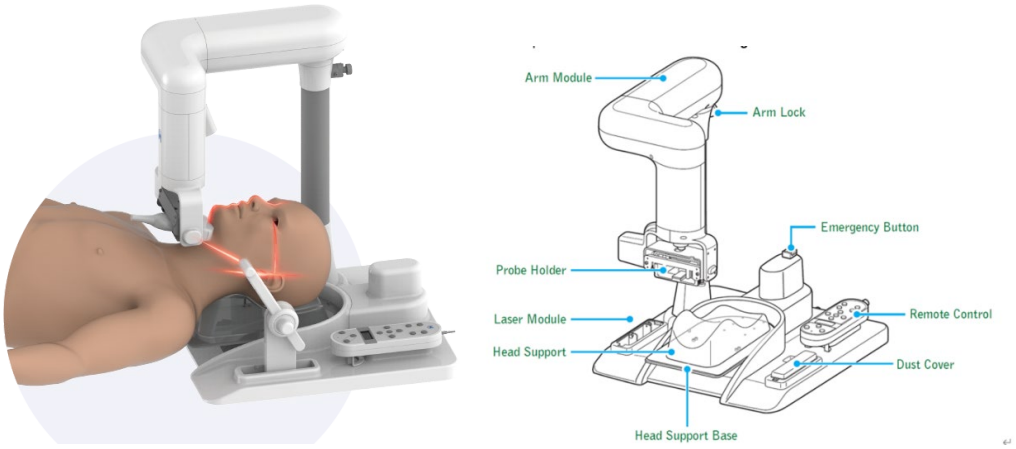


Figure 2: Patient positioned in Am-CAD UO unit, prior to ultrasound scan (left). The entire Am-CAD UO set-up, where the patient lays flat and is positioned in the unit (right)



DocuSign Envelope ID: FF917FA4-BEA0-4E08-96D0-A9016C337F14

Figure 3: Resulting image when the patient is properly positioned in the Am-CAD unit and scan is initiated. Top of the image is anterior, with the bottom of the image posterior. The bright white line is the airway.

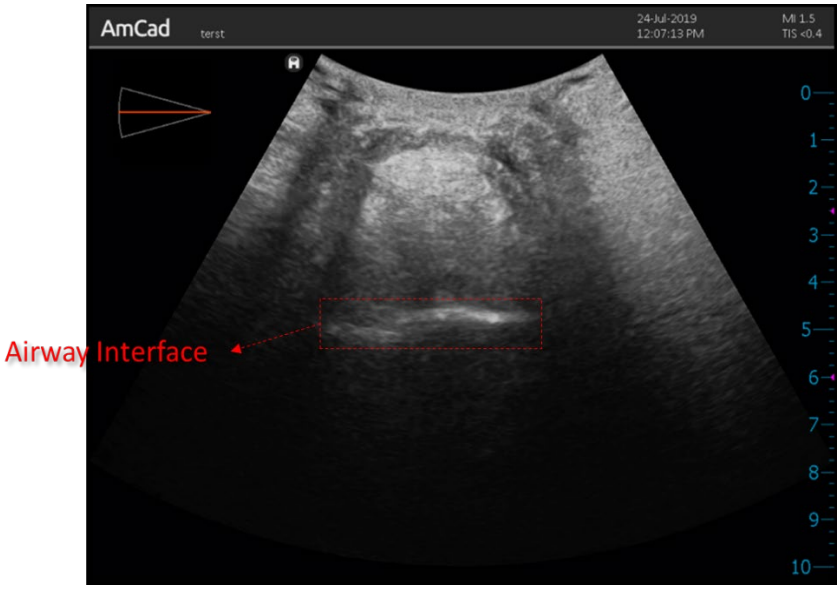


Figure 4: Ultrasound Tablet and Ultrasound Probe for the Am-CAD UO unit. The tablet displays the ultrasound image in real time.



DocuSign Envelope ID: FF917FA4-BEA0-4E08-96D0-A9016C337F14

Figure 5: Depiction of what regions of the airway velum, oropharynx, tongue base, and epiglottis correspond to.

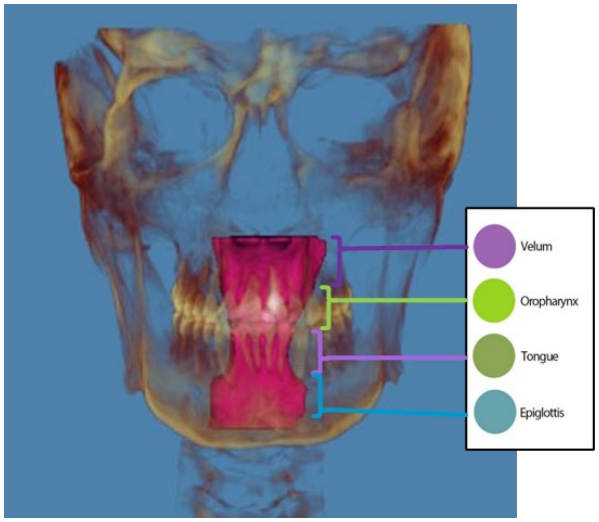
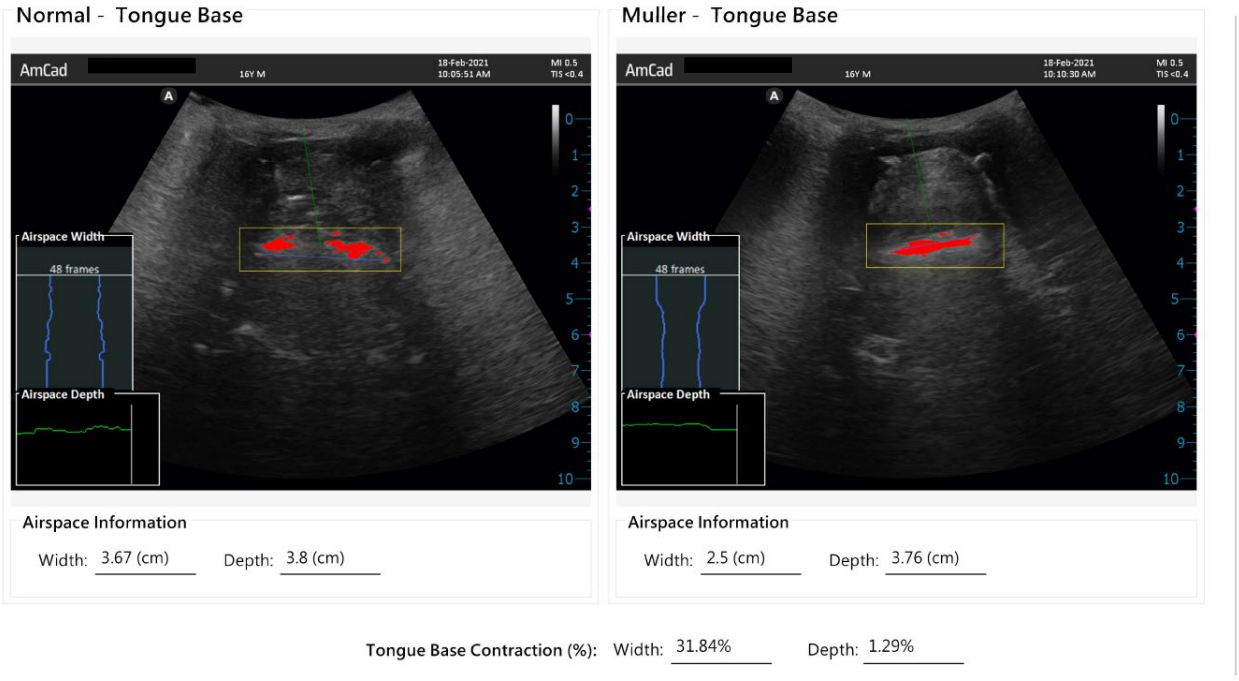


Figure 6: Depiction of airspace identification between normal breathing and Muller maneuver. In this example, the subject showed 31.84% lateral collapse of the airway at the tongue base with Muller maneuver. Red shading is what the software defines as airspace, with the blue line representing the width of the airspace.



DocuSign Envelope ID: FF917FA4-BEA0-4E08-96D0-A9016C337F14

Figure 7: Lateral airspace contraction (collapse) at Velum, Oropharynx, Tongue Base, and Epiglottis for subjects 1-9

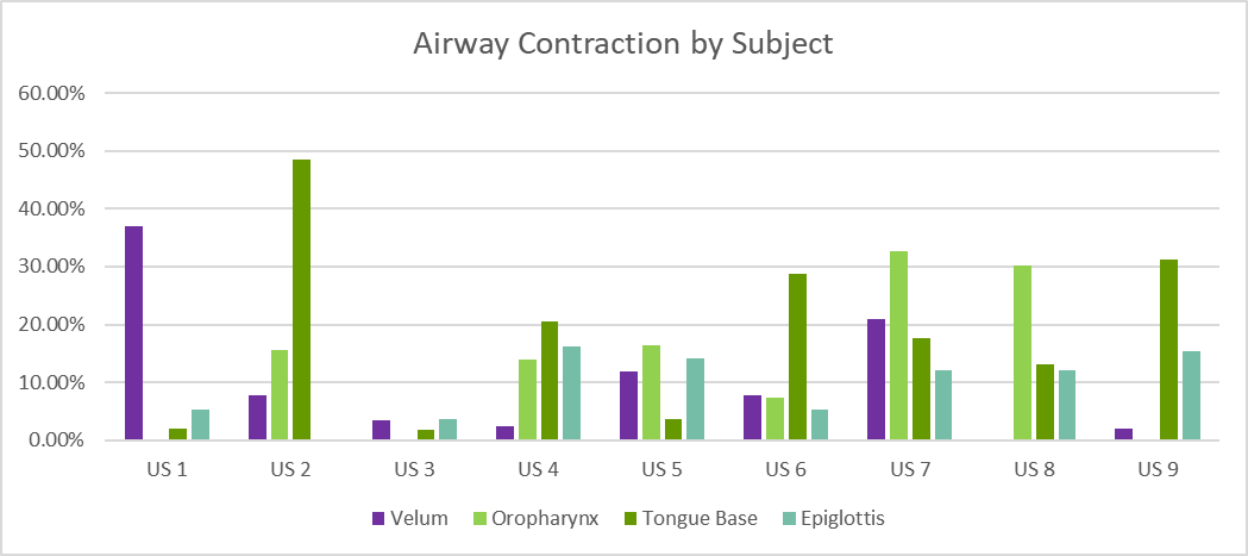
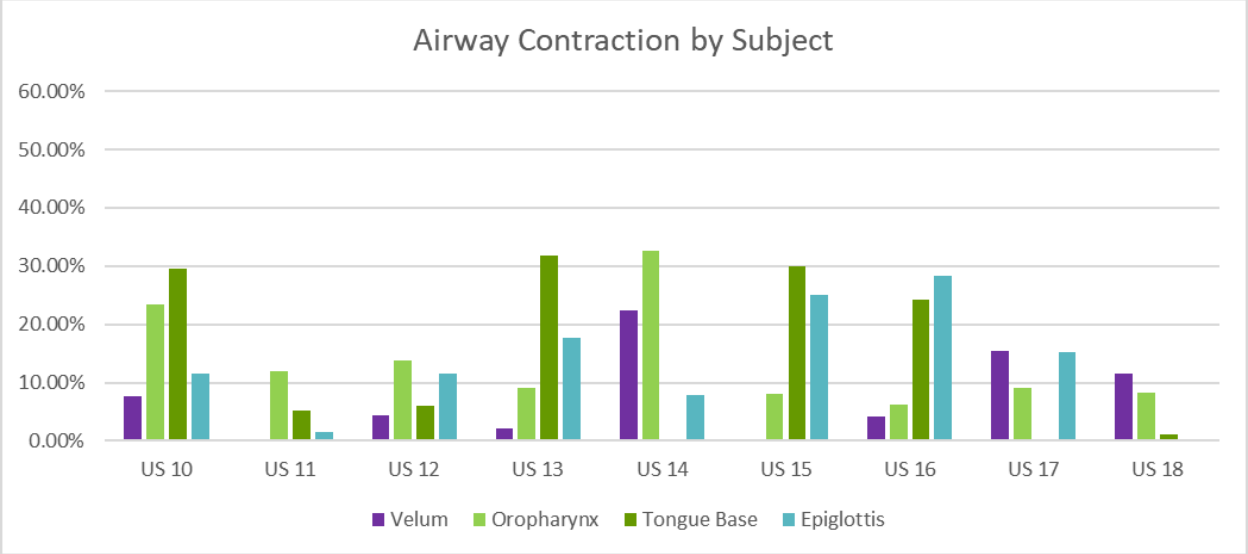


Figure 8: Lateral airspace contraction (collapse) at Velum, Oropharynx, Tongue Base, and Epiglottis for subjects 10-18



DocuSign Envelope ID: FF917FA4-BEA0-4E08-96D0-A9016C337F14

Figure 9: 4 scans that were previously repeated to confirm the patient's OSA risk assessment. Total collapse was similar for all but US17. The area of greatest collapse also changed with repeated scans.

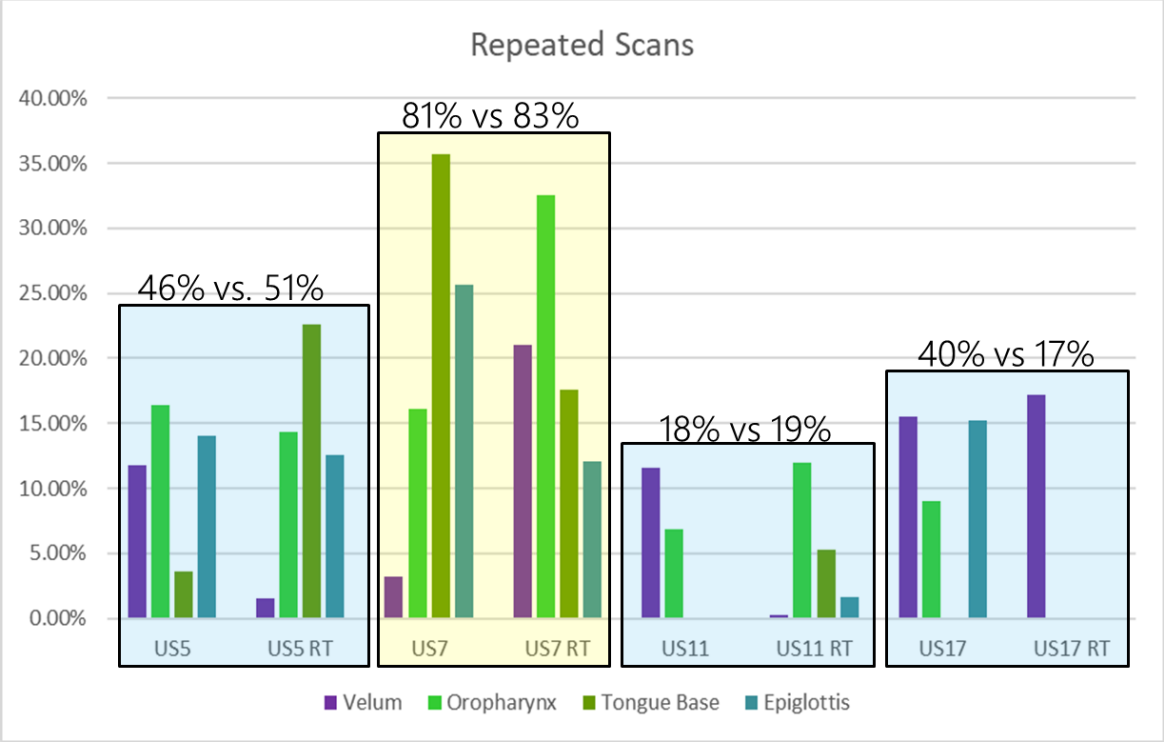
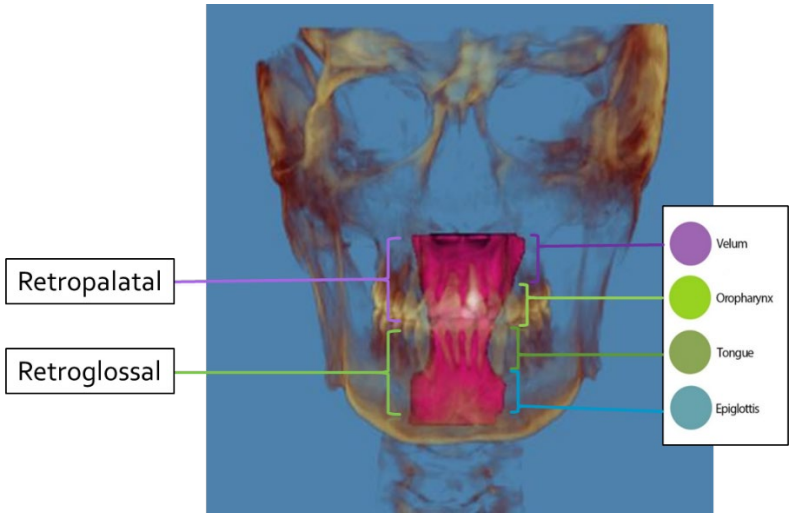


Figure 10: Diagram showing how the locations of velum, oropharynx, tongue base, and epiglottis correspond to retropalatal and retroglossal regions



DocuSign Envelope ID: FF917FA4-BEA0-4E08-96D0-A9016C337F14

MANUSCRIPT REFERENCES

1. Abtahi S, Witmans M, Alsufyani NA, Major MP, Major PW. Pediatric sleep-disordered breathing in the orthodontic population: Prevalence of positive risk and associations. *American Journal of Orthodontics and Dentofacial Orthopedics*. 2020; 157(4).

2. Kryger MH. Diagnosis and management of sleep apnea syndrome. *Clinical Cornerstone*. 2000; 2(5): 39-44.

3. Semelka M, Wilson J, Floyd R. Diagnosis and Treatment of Obstructive Sleep Apnea in Adults. *American Family Physician*. 2016; 94(5): 355-360.

4. D'Agostino MA. Obstructive sleep apnea, diagnosis, management, and treatment. *Otolaryngologic Clinics of North America*. 2016; 49(6): xiii-xiv.

5. Lumeng JC, Chervin RD. Epidemiology of pediatric obstructive sleep apnea. *Proceedings of the American Thoracic Society*. 2008; 5(2): 242-252.

6. Rohra AK, Demko CA, Hans MG, Rosen C, Palomo JM. Sleep disordered breathing in children seeking orthodontic care. *American Journal of Orthodontics and Dentofacial Orthopedics*. 2018; 154(1): 65-71.

7. Gipson K, Lu M, Kinane TB. Sleep-disordered breathing in children. *Pediatrics in Review*. 2019; 40(1): 3-13.

8. Huang Y, Guilleminault C. Pediatric obstructive sleep apnea: Where do we stand? *Sleep-Related Breathing Disorders*. 2017; 136-144.

9. Guilleminault C, Korohkin R, Winkle R. A review of 50 children with obstructive sleep apnea syndrome. *Lung*. 1981; 159: 275-287.

10. Savini S, Ciorba A, Bianchini C, Stomeo F, Corazzi V, Vicini C, Pelucchi S. Assessment of obstructive sleep apnea (osa) in

DocuSign Envelope ID: FF917FA4-BEA0-4E08-96D0-A9016C337F14

children: An update. *Acta Otorhinolaryngologica Italica*. 2019; 39(5): 289-297.

11. Behrents RG, Shelgikar AV, Conley RS, Flores-Mir C, Hans MG, Levine M, Palomo JM, Hittner J. Obstructive sleep apnea and orthodontics: An American Association of Orthodontists white paper. *American Journal of Orthodontics and Dentofacial Orthopedics*. 2019; 156(1).

12. Chandrakantan, A., Musso, M. F., Floyd, T., & Adler, A. C. (2020). Pediatric obstructive sleep apnea: Preoperative and neurocognitive considerations for perioperative management. Pediatric Anesthesia, 30(5), 529-536. doi:10.1111/pan.13855

13. Greig SR. Current perspectives on the role of tonsillectomy. *Journal of Paediatrics and Child Health*. 2017; 53(11): 1065-1070.

14. Guilleminault C, Hill MW, Simmons F, Dement WC. Obstructive sleep apnea: Electromyographic and fiberoptic studies. *Experimental Neurology*. 1978; 62(1): 48-67.

15. Choi D, Bae J, Hu K, Kim H. Anatomical variations of the stylopharyngeus and superior constrictors in relation to their function. *Anatomy & Cell Biology*. 2020; 53(4): 417-421.

16. Dewald D. Why are the tonsils in the airway? Revisiting the pathophysiology of tonsillar airway obstruction. Paper presented at: IPSA Online: The 6th congress of the International Pediatric Sleep Association; February 5-6, 2021, 2021.

17. Arens R, Sin S, McDonough JM, Palmer JM, Dominguez T, Meyer, H, Pack AI. Changes in upper airway size during tidal breathing in children with obstructive sleep apnea syndrome. *American Journal of Respiratory and Critical Care Medicine*. 2005; 171(11): 1298-1304.

18. Dewald D. Pharyngeal anatomy. University Hospitals, 28 May 2021, Cleveland, Ohio. Lecture.

DocuSign Envelope ID: FF917FA4-BEA0-4E08-96D0-A9016C337F14

19. Yu JL, Afolabi-Brown O. Updates on management of pediatric obstructive sleep apnea. *Pediatric Investigation*. 2019; 3(4): 228-235.

20. Quinlan CM, Otero H, Tapia IE. Upper airway visualization in pediatric obstructive sleep apnea. *Paediatric Respiratory Reviews*. 2019; 32: 48-54.

21. Nayak KS, Fleck RJ. Seeing sleep: Dynamic imaging of upper airway collapse and collapsibility in children. *IEEE Pulse*. 2014; 5(5): 40-44.

22. Shu C, Lee P, Lin J, Huang C, Chang Y, Yu C, Wang H. The use of sub-mental ultrasonography for identifying patients with severe obstructive sleep apnea. *PLoS ONE*. 2013; 8(5).

23. Ronen O, Malhotra A, Pillar G. Influence of gender and age on upper-airway length during development. *Pediatrics*. 2007; 120(4): 1028-1034.

24. Enlow D, Hans MG. Essentials of Facial Growth. TMData Resources; 2008.

DocuSign Envelope ID: FF917FA4-BEA0-4E08-96D0-A9016C337F14

APPENDICES

Appendix A: IRB Approval

IRB Administration Offices
UH IRB Phone: 216.844.1529
CWRU IRB Phone: 216.368.6925

INITIAL APPROVAL

Principal Investigator:	Mark Hans
Title:	Comparison of airway collapsibility in children with signs and symptoms of sleep disordered breathing using submental ultrasound
Submission Number:	STUDY20201128
IRB Office:	CWRU IRB
Approval Date:	3/23/2021
Effective Date:	3/23/2021
Approval End Date	N/A
Type of Submission:	Initial Study
Type of Review:	Expedited
Documents Reviewed:	• Data Collection Sheet, Category: Other; • IRB HIPAA Waiver Form with Clarifications, Category: IRB Protocol; • IRB Protocol with clarifications, Category: IRB Protocol

The IRB has reviewed this submission.

- Per Federal regulation, changes MAY NOT be made to any element of the current research without prior IRB approval, except to eliminate an immediate and apparent hazard to subjects enrolled in the study.
- Per Federal regulation, the research may not continue beyond the Approval End date. You must submit a continuing review form 6-8 weeks before this Approval End date in order to maintain IRB approval. Failure to maintain IRB approval is human subjects non-compliance. Please note that even if your study falls into a category that does not require an Approval End date, the institution may require a yearly "check-in" to confirm the status of the study.

***Approval by the IRB does NOT mean that you have permission to start your study. Prior to starting your study, you may be required to obtain (1) a coverage analysis for studies that involve patient care, regardless of source of funding, and/or (2) a contract with the Sponsor of your study or an agreement with any third-party collaborator that may receive UH or CWRU patient information in any format. Please ensure that all required approvals are obtained before initiation of research activity. ***

The UH IRB operates under HHS Federalwide Assurance (FWA) number 00003937 and IRB registration numbers 00000684, 00001691 and 00008600. The CWRU IRB operates under DHHS FWA00004428 and IRB registration number 00000683.

HRP-510

Page 1 of 1

DocuSign Envelope ID: FF917FA4-BEA0-4E08-96D0-A9016C337F14

Appendix B: Abbreviation Key

SDB: Sleep Disordered Breathing

OSA: Obstructive Sleep Apnea

US: Ultrasound

CWRU: Case Western Reserve University

DocuSign Envelope ID: FF917FA4-BEA0-4E08-96D0-A9016C337F14

Appendix C: Airspace Contraction (collapse) and Tongue Thickness Summary per Subject

US1

Airspace Width (cm)

	Tidal Breathing			Müller's Maneuver			Contraction (%)
	Max	Median	Min	Max	Median	Min	
Velum	3.8	3.4	1.75	2.66	2.14	1	36.89%
Oropharynx	3.08	2.35	2.06	3.02	2.72	1.66	None
Tongue Base	3.46	3.04	2.65	3.37	2.98	1.78	2.04%
Epiglottis	3.24	2.89	2.77	3.09	2.74	2.66	5.22%

Tongue Thickness (cm)

	Tidal Breathing			Müller's Maneuver			Change (%)
	Max	Median	Min	Max	Median	Min	
Velum	3.47	3.39	2.86	4.03	3.57	3.41	-5.28%
Oropharynx	3.63	3.01	2.67	3.26	3.22	2.84	-7.02%
Tongue Base	3.06	2.58	2.24	3.25	2.83	2.56	-9.62%
Epiglottis	3.15	2.78	2.73	3.14	3.01	2.59	-8.13%

US2

Airspace Width (cm)

	Tidal Breathing			Müller's Maneuver			Contraction (%)
	Max	Median	Min	Max	Median	Min	
Velum	4.3	3.83	3.36	3.67	3.53	1.69	7.85%
Oropharynx	4.28	3.87	2.89	3.39	3.27	2.62	15.52%
Tongue Base	4.08	3.67	2.75	3.07	1.89	1.6	48.42%
Epiglottis	1.75	1.53	1.25	2.3	1.6	0.78	None

Tongue Thickness (cm)

	Tidal Breathing			Müller's Maneuver			Change (%)
	Max	Median	Min	Max	Median	Min	
Velum	4.59	3.99	3.45	4.33	4.09	3.47	-2.38%
Oropharynx	3.76	3.28	2.89	3.47	2.98	2.54	8.91%
Tongue Base	3.52	3	2.53	3.68	3.13	2.55	-4.4%
Epiglottis	4.34	4.17	3.95	4.53	4.19	3.87	-0.53%

US3

DocuSign Envelope ID: FF917FA4-BEA0-4E08-96D0-A9016C337F14

Airspace Width (cm)

	Tidal Breathing			Müller's Maneuver			Contraction (%)
	Max	Median	Min	Max	Median	Min	
Velum	4.49	3.91	3.83	4.19	3.78	3.71	3.45%
Oropharynx	4.35	3.84	2.7	4.07	3.88	2.31	None
Tongue Base	3.54	3.16	2.86	3.34	3.11	2.92	1.71%
Epiglottis	3.24	3.15	3.04	3.16	3.04	2.78	3.59%

Tongue Thickness (cm)

	Tidal Breathing			Muller's Maneuver			Change (%)
	Max	Median	Min	Max	Median	Min	
Velum	4.38	4.28	3.98	4.63	4.57	4.3	-6.7%
Oropharynx	4.14	3.97	3.75	4.22	4	3.86	-0.55%
Tongue Base	3.92	3.82	3.56	4.03	3.92	3.71	-2.51%
Epiglottis	4.11	3.7	3.46	4.05	3.84	3.53	-3.81%

US4

Airspace Width (cm)

	Tidal Breathing			Müller's Maneuver			Contraction (%)
	Max	Median	Min	Max	Median	Min	
Velum	4.09	3.88	3.44	4.06	3.79	3.22	2.4%
Oropharynx	4.17	3.67	3.28	3.65	3.16	2.78	13.91%
Tongue Base	3.52	3.05	1.91	3.47	2.42	1.39	20.54%
Epiglottis	2.93	2.83	2.04	3.15	2.37	1.91	16.18%

Tongue Thickness (cm)

	Tidal Breathing			Muller's Maneuver			Change (%)
	Max	Median	Min	Max	Median	Min	
Velum	5.77	5.26	4.96	5.48	5.21	4.86	0.95%
Oropharynx	5.81	5.37	4.78	5.72	5.28	5.16	1.73%
Tongue Base	5.61	5.22	4.98	4.8	4.64	4.22	11.12%
Epiglottis	5.14	5.01	4.8	4.96	4.56	4.31	9.17%

US5

DocuSign Envelope ID: FF917FA4-BEA0-4E08-96D0-A9016C337F14

Airspace Width (cm)

	Tidal Breathing			Müller's Maneuver			Contraction (%)
	Max	Median	Min	Max	Median	Min	
Velum	5.57	4.94	4.73	5.05	4.87	4.5	1.5%
Oropharynx	4.54	4.29	3.72	4.18	3.67	3.18	14.35%
Tongue Base	4.29	3.88	3.37	3.62	3	2.48	22.58%
Epiglottis	4.46	3.67	3.6	4.38	3.21	2.75	12.58%

Tongue Thickness (cm)

	Tidal Breathing			Müller's Maneuver			Change (%)
	Max	Median	Min	Max	Median	Min	
Velum	4.72	4.68	4.56	5.44	5.07	4.79	-8.13%
Oropharynx	4.81	4.44	4.36	4.75	4.58	4.11	-3.13%
Tongue Base	4.48	4.2	4.15	4.44	4.28	4	-1.98%
Epiglottis	4.01	3.96	3.89	4.41	4.36	4.12	-10.15%

US6

Airspace Width (cm)

	Tidal Breathing			Müller's Maneuver			Contraction (%)
	Max	Median	Min	Max	Median	Min	
Velum	5.7	5.21	4.96	5.34	4.8	4.21	7.84%
Oropharynx	5.82	5.62	5.36	5.75	5.21	4.66	7.31%
Tongue Base	5.87	5.42	3.51	4.55	3.86	3.34	28.85%
Epiglottis	5.13	3.78	3.54	3.89	3.58	2.67	5.31%

Tongue Thickness (cm)

	Tidal Breathing			Müller's Maneuver			Change (%)
	Max	Median	Min	Max	Median	Min	
Velum	6.11	5.82	5.52	6.18	5.81	5.37	0.33%
Oropharynx	5.69	5.51	5.1	5.84	5.57	5.25	-1.07%
Tongue Base	5.86	5.33	5.09	5.92	5.48	5.24	-2.83%
Epiglottis	5.54	5.37	5.05	5.43	5.27	4.98	1.88%

US7

DocuSign Envelope ID: FF917FA4-BEA0-4E08-96D0-A9016C337F14

Airspace Width (cm)

	Tidal Breathing			Müller's Maneuver			Contraction (%)
	Max	Median	Min	Max	Median	Min	
Velum	4.12	3.74	3.15	3.28	2.96	2.75	21%
Oropharynx	4.16	3.4	2.78	2.97	2.29	2.05	32.59%
Tongue Base	3.47	3.22	3.07	3.59	2.65	1.3	17.54%
Epiglottis	3.82	3.22	2.88	2.94	2.84	2.51	12.04%

Tongue Thickness (cm)

	Tidal Breathing			Müller's Maneuver			Change (%)
	Max	Median	Min	Max	Median	Min	
Velum	6.19	5.97	5.71	5.96	5.79	5.38	3.05%
Oropharynx	5.75	5.57	5.07	5.8	5.31	5.15	4.76%
Tongue Base	5.14	4.81	4.68	5.3	5.01	4.72	-4.33%
Epiglottis	5.11	4.43	3.97	5.04	4.58	4.52	-3.43%

US8

Airspace Width (cm)

	Tidal Breathing			Müller's Maneuver			Contraction (%)
	Max	Median	Min	Max	Median	Min	
Velum	4.38	4.05	4	4.59	4.34	4.1	None
Oropharynx	4.86	4.22	3.25	3.65	2.94	2.46	30.27%
Tongue Base	3.37	3	2.75	3.09	2.61	2.1	13.13%
Epiglottis	3.21	2.9	2.78	2.74	2.55	2.04	12.09%

Tongue Thickness (cm)

	Tidal Breathing			Müller's Maneuver			Change (%)
	Max	Median	Min	Max	Median	Min	
Velum	5.19	5.11	4.64	5.28	4.79	4.67	6.3%
Oropharynx	5.14	4.76	4.31	5.02	4.55	4.35	4.48%
Tongue Base	4.86	4.62	4.34	4.65	4.46	4.34	3.48%
Epiglottis	4.72	4.43	4.35	4.77	4.52	4.03	-2.08%

US9

DocuSign Envelope ID: FF917FA4-BEA0-4E08-96D0-A9016C337F14

Airspace Width (cm)

	Tidal Breathing			Müller's Maneuver			Contraction (%)
	Max	Median	Min	Max	Median	Min	
Velum	1.78	1.54	0.89	2.02	1.5	1.3	2.02%
Oropharynx	4.89	1.5	1.26	4.4	2.62	1.31	None
Tongue Base	4.93	4.53	2.69	3.71	3.11	1.23	31.18%
Epiglottis	4.47	3.65	2.98	3.71	3.09	1.15	15.34%

Tongue Thickness (cm)

	Tidal Breathing			Müller's Maneuver			Change (%)
	Max	Median	Min	Max	Median	Min	
Velum	5.56	5.35	5.07	5.67	5.38	5.16	-0.64%
Oropharynx	5.4	5.18	4.9	5.3	4.88	4.8	5.79%
Tongue Base	5.14	4.95	4.76	5.04	4.92	4.88	0.55%
Epiglottis	4.94	4.88	4.27	5.29	4.8	4.4	1.6%

US10

Airspace Width (cm)

	Tidal Breathing			Müller's Maneuver			Contraction (%)
	Max	Median	Min	Max	Median	Min	
Velum	4.37	3.99	3.74	4.07	3.69	3.49	7.57%
Oropharynx	4.1	3.96	3.79	3.29	3.03	2.62	23.45%
Tongue Base	3.76	3.4	3.1	2.99	2.4	2.2	29.48%
Epiglottis	3.86	3.25	2.25	3.24	2.87	1.81	11.58%

Tongue Thickness (cm)

	Tidal Breathing			Müller's Maneuver			Change (%)
	Max	Median	Min	Max	Median	Min	
Velum	4.45	4.15	3.61	3.88	3.8	3.72	8.47%
Oropharynx	3.72	3.42	3.39	3.72	3.6	3.49	-5.18%
Tongue Base	3.48	3.42	3.37	3.62	3.57	3.42	-4.29%
Epiglottis	3.6	3.59	3.5	3.88	3.7	3.59	-3.09%

US11

DocuSign Envelope ID: FF917FA4-BEA0-4E08-96D0-A9016C337F14

Airspace Width (cm)

	Tidal Breathing			Müller's Maneuver			Contraction (%)
	Max	Median	Min	Max	Median	Min	
Velum	4.61	4.14	4.01	4.26	4.13	3.54	0.27%
Oropharynx	4.26	3.6	3.21	3.43	3.16	2.68	12.01%
Tongue Base	4.19	3.05	2.24	3.39	2.89	2.39	5.25%
Epiglottis	2.97	2.73	2.05	2.86	2.69	2.14	1.61%

Tongue Thickness (cm)

	Tidal Breathing			Müller's Maneuver			Change (%)
	Max	Median	Min	Max	Median	Min	
Velum	4.3	3.95	3.83	3.9	3.88	3.38	1.7%
Oropharynx	3.96	3.42	3.27	3.57	3.34	3.1	2.19%
Tongue Base	3.49	3.38	3.21	3.64	3.41	3.23	-0.74%
Epiglottis	3.43	3.23	3.18	3.52	3.42	3.17	-5.85%

US12

Airspace Width (cm)

	Tidal Breathing			Müller's Maneuver			Contraction (%)
	Max	Median	Min	Max	Median	Min	
Velum	3.95	3.27	2.87	3.14	3.13	2.16	4.43%
Oropharynx	3.22	2.91	1.76	2.89	2.51	1.6	13.7%
Tongue Base	3	2.87	2.64	3.06	2.7	1.48	6.12%
Epiglottis	3.35	3.13	2.73	3.06	2.77	2.3	11.56%

Tongue Thickness (cm)

	Tidal Breathing			Müller's Maneuver			Change (%)
	Max	Median	Min	Max	Median	Min	
Velum	4.18	4.07	3.76	3.6	3.55	3.08	12.85%
Oropharynx	3.88	3.26	3.18	3.81	3.49	3.14	-6.99%
Tongue Base	3.24	2.96	2.9	3.67	2.98	2.89	-0.78%
Epiglottis	3.44	3.09	2.85	3.28	3.02	2.77	2.55%

US13

DocuSign Envelope ID: FF917FA4-BEA0-4E08-96D0-A9016C337F14

Airspace Width (cm)

	Tidal Breathing			Müller's Maneuver			Contraction (%)
	Max	Median	Min	Max	Median	Min	
Velum	4.47	4.13	4.06	4.2	4.04	3.56	2.23%
Oropharynx	4.41	4	2.84	4.08	3.64	2.21	9.04%
Tongue Base	4.02	3.67	3.16	3.4	2.5	2.21	31.84%
Epiglottis	4	3.76	3.07	3.28	3.1	2.16	17.59%

Tongue Thickness (cm)

	Tidal Breathing			Müller's Maneuver			Change (%)
	Max	Median	Min	Max	Median	Min	
Velum	5.39	4.57	3.94	5.02	4.76	4.52	-4.29%
Oropharynx	4.37	4.2	3.85	4.33	3.95	3.62	5.95%
Tongue Base	3.96	3.8	3.69	4.1	3.76	3.7	1.29%
Epiglottis	4.15	3.86	3.74	4.12	4.09	3.91	-5.72%

US14

Airspace Width (cm)

	Tidal Breathing			Müller's Maneuver			Contraction (%)
	Max	Median	Min	Max	Median	Min	
Velum	2.97	2.94	2.81	2.8	2.28	1.34	22.29%
Oropharynx	3.53	3.22	2.85	2.75	2.18	1.67	32.53%
Tongue Base	3.38	2.93	1.94	3.23	3.07	1.14	None
Epiglottis	1.98	1.84	1.18	2.37	1.7	1.4	7.87%

Tongue Thickness (cm)

	Tidal Breathing			Müller's Maneuver			Change (%)
	Max	Median	Min	Max	Median	Min	
Velum	4.03	3.92	3.85	4.44	4.42	4.33	-12.9%
Oropharynx	4.22	3.89	3.71	4.54	4.28	4.24	-10.13%
Tongue Base	3.89	3.63	3.26	4.27	4.17	3.8	-15.05%
Epiglottis	4.1	4	3.51	4.44	4.27	3.97	-6.8%

US15

DocuSign Envelope ID: FF917FA4-BEA0-4E08-96D0-A9016C337F14

Airspace Width (cm)

	Tidal Breathing			Müller's Maneuver			Contraction (%)
	Max	Median	Min	Max	Median	Min	
Velum	3.54	2.85	1.89	3.39	2.87	1.96	None
Oropharynx	3.08	2.63	2.24	2.86	2.41	1.81	8.07%
Tongue Base	3.05	2.77	2.45	2.54	1.94	1.51	30.05%
Epiglottis	3.04	2.76	2.19	3	2.07	1.45	24.96%

Tongue Thickness (cm)

	Tidal Breathing			Müller's Maneuver			Change (%)
	Max	Median	Min	Max	Median	Min	
Velum	4.91	4.88	4.54	5.46	5.16	4.82	-5.78%
Oropharynx	4.76	4.43	4.35	4.91	4.62	4.26	-4.34%
Tongue Base	4.4	4.16	4.05	4.68	4.53	4.21	-8.85%
Epiglottis	4.42	4.14	3.91	4.6	4.38	4.19	-5.87%

US16

Airspace Width (cm)

	Tidal Breathing			Müller's Maneuver			Contraction (%)
	Max	Median	Min	Max	Median	Min	
Velum	3.1	2.9	2.18	2.97	2.78	2.57	4.23%
Oropharynx	2.86	2.64	0.99	3.07	2.48	2.2	6.28%
Tongue Base	2.31	2.02	1.76	1.87	1.53	1.13	24.16%
Epiglottis	2.62	2.53	2.48	2.28	1.81	1.29	28.35%

Tongue Thickness (cm)

	Tidal Breathing			Müller's Maneuver			Change (%)
	Max	Median	Min	Max	Median	Min	
Velum	3.84	3.47	3.44	3.84	3.64	3.58	-4.81%
Oropharynx	3.88	3.26	2.82	3.67	3.37	3.06	-3.34%
Tongue Base	3.3	3.16	2.7	3.58	3.3	2.74	-4.4%
Epiglottis	2.78	2.71	2.48	3.65	3.22	2.75	-18.85%

US17

DocuSign Envelope ID: FF917FA4-BEA0-4E08-96D0-A9016C337F14

Airspace Width (cm)

	Tidal Breathing			Müller's Maneuver			Contraction (%)
	Max	Median	Min	Max	Median	Min	
Velum	5.72	5.66	5.32	4.94	4.68	4.42	17.17%
Oropharynx	5.35	4.42	4.23	4.62	4.43	4.27	None
Tongue Base	4.95	4.18	3.92	4.81	4.49	4.1	None
Epiglottis	3.69	3.59	3.44	4.24	3.96	3.6	None

Tongue Thickness (cm)

	Tidal Breathing			Müller's Maneuver			Change (%)
	Max	Median	Min	Max	Median	Min	
Velum	5.16	4.94	4.94	5.23	4.71	4.61	4.67%
Oropharynx	5.12	4.78	4.47	4.75	4.58	4.43	4.08%
Tongue Base	4.91	4.43	4.12	4.57	4.38	4.22	1.06%
Epiglottis	4.27	3.92	3.84	4.23	4.17	3.78	-6.4%

US18

Airspace Width (cm)

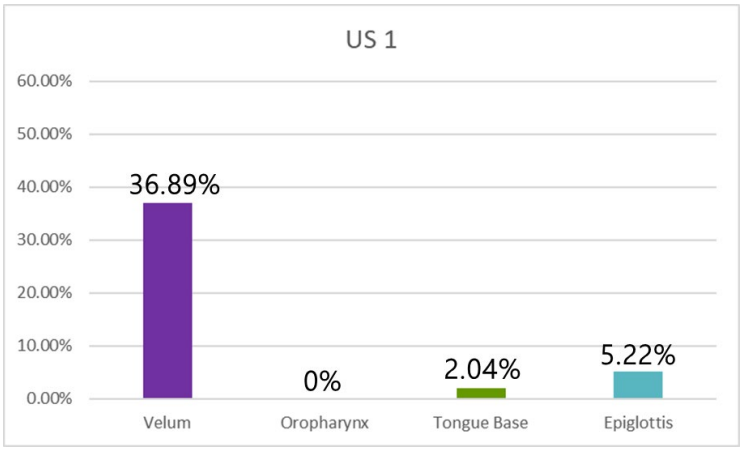
	Tidal Breathing			Müller's Maneuver			Contraction (%)
	Max	Median	Min	Max	Median	Min	
Velum	5.04	4.41	4.28	4.12	3.9	3.83	11.58%
Oropharynx	4.08	3.88	3.21	3.66	3.56	3.16	8.25%
Tongue Base	3.74	3.51	3.26	3.62	3.47	2.76	1.05%
Epiglottis	3.33	2.73	2.62	4.14	2.86	2.42	None

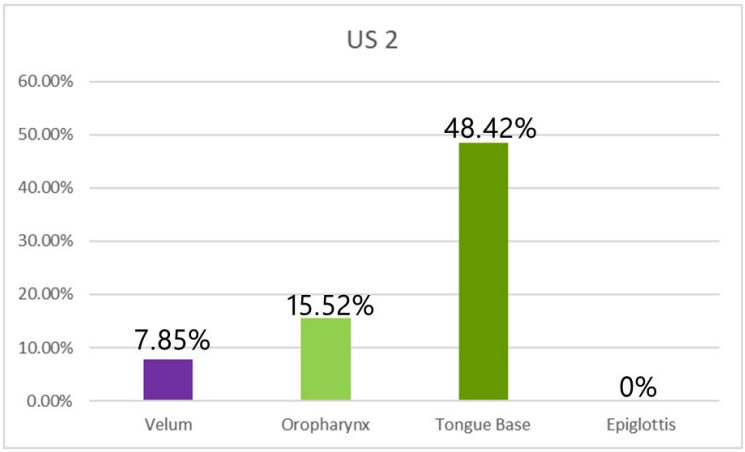
Tongue Thickness (cm)

	Tidal Breathing			Müller's Maneuver			Change (%)
	Max	Median	Min	Max	Median	Min	
Velum	3.81	3.64	3.57	4.17	3.74	3.57	-2.53%
Oropharynx	3.71	3.42	3.07	3.81	3.6	3.37	-5.41%
Tongue Base	3.41	3.27	3.17	3.71	3.46	3.15	-5.68%
Epiglottis	3.03	2.98	2.92	3.86	3.75	3.32	-25.87%

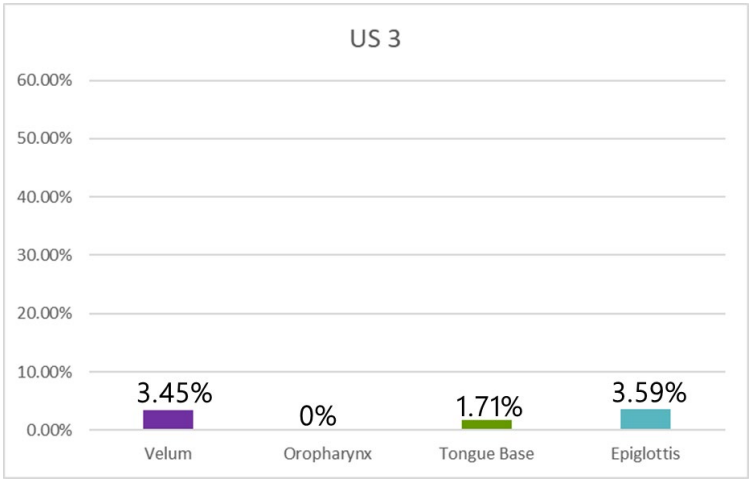
DocuSign Envelope ID: FF917FA4-BEA0-4E08-96D0-A9016C337F14

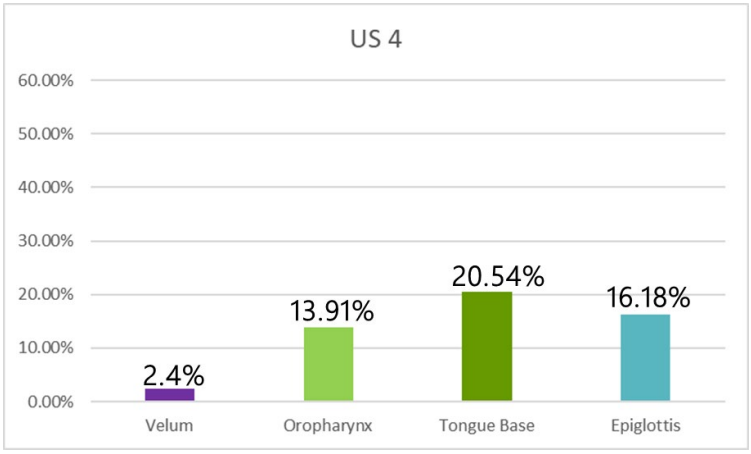
Appendix D: Graphical Depiction of Airway Contraction (Collapse) For Each Subject

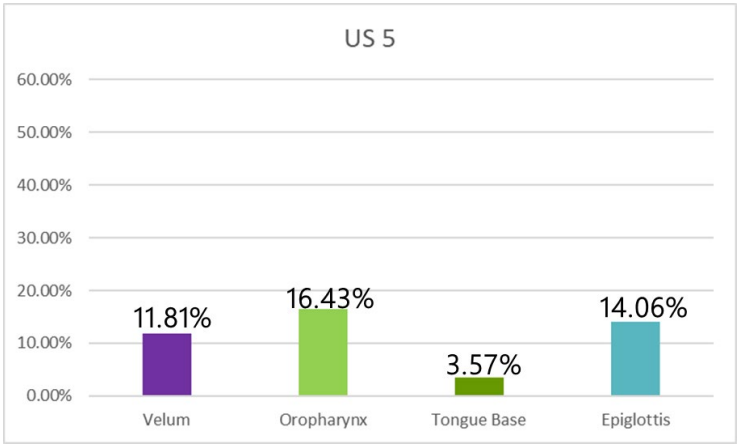




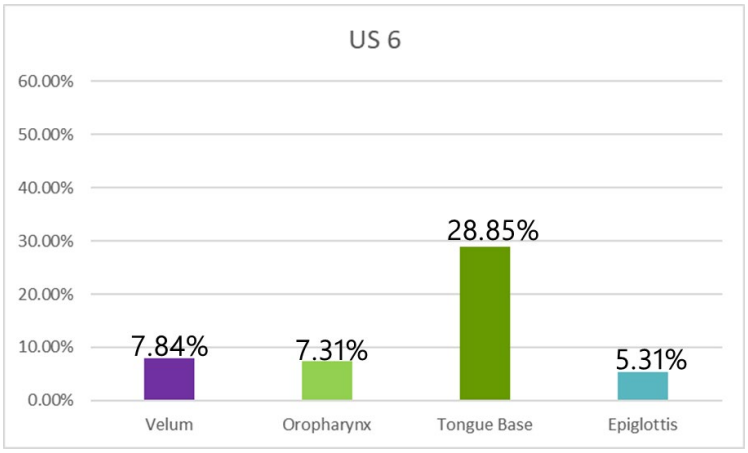
DocuSign Envelope ID: FF917FA4-BEA0-4E08-96D0-A9016C337F14

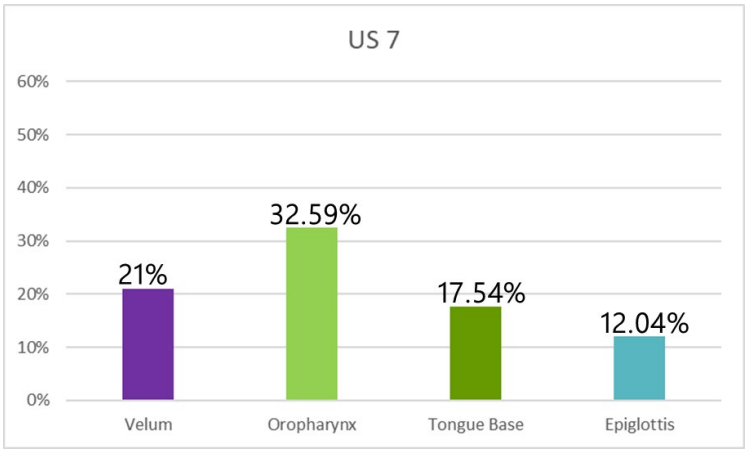


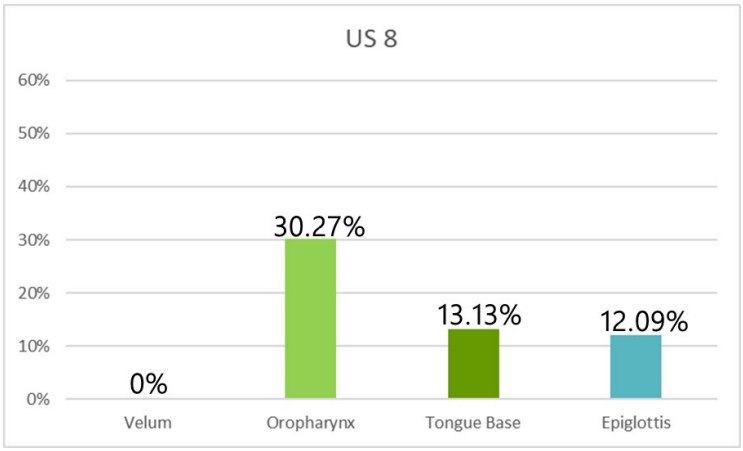




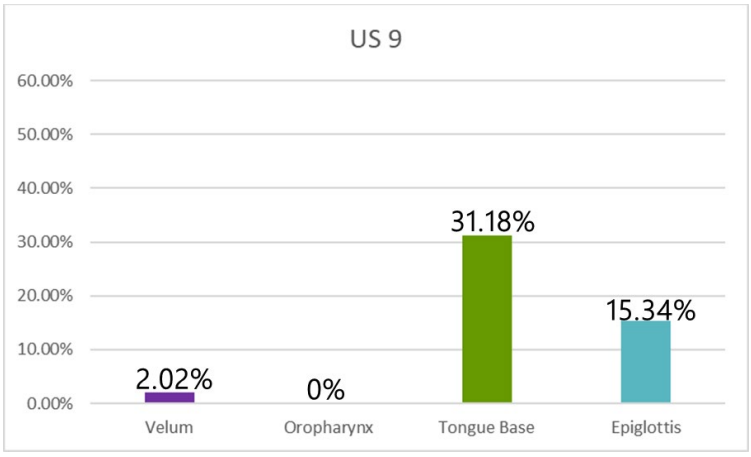
DocuSign Envelope ID: FF917FA4-BEA0-4E08-96D0-A9016C337F14

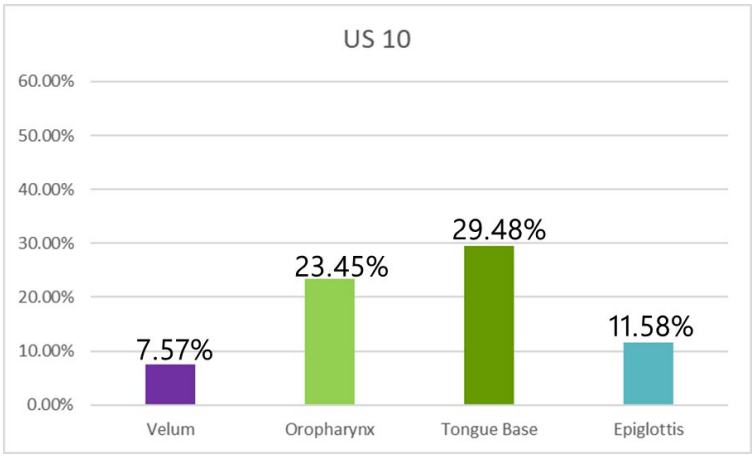


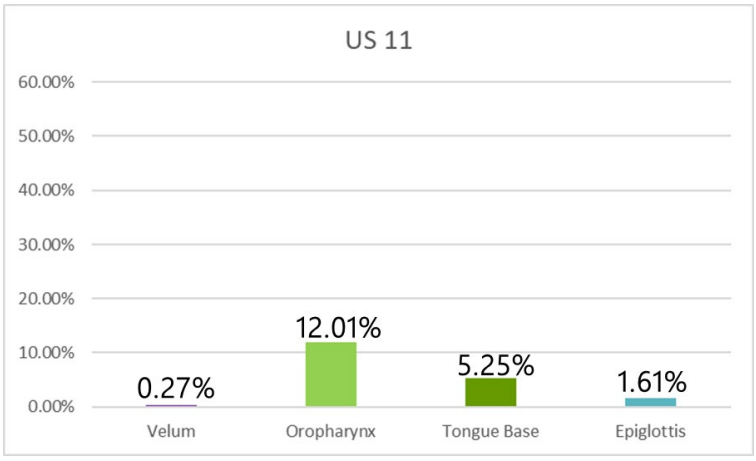




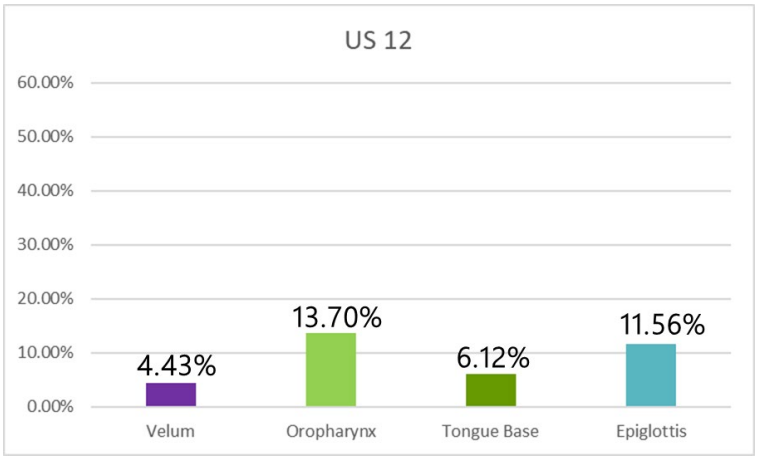
DocuSign Envelope ID: FF917FA4-BEA0-4E08-96D0-A9016C337F14

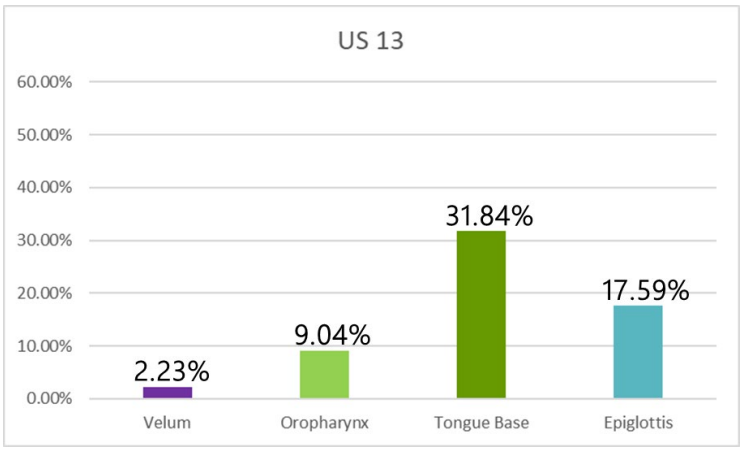


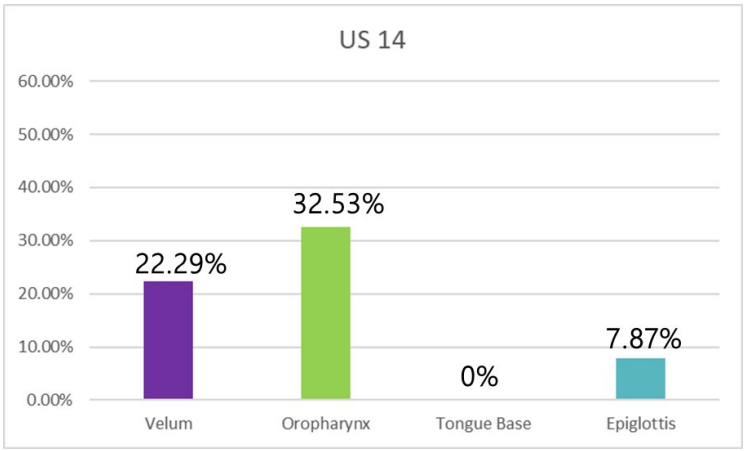




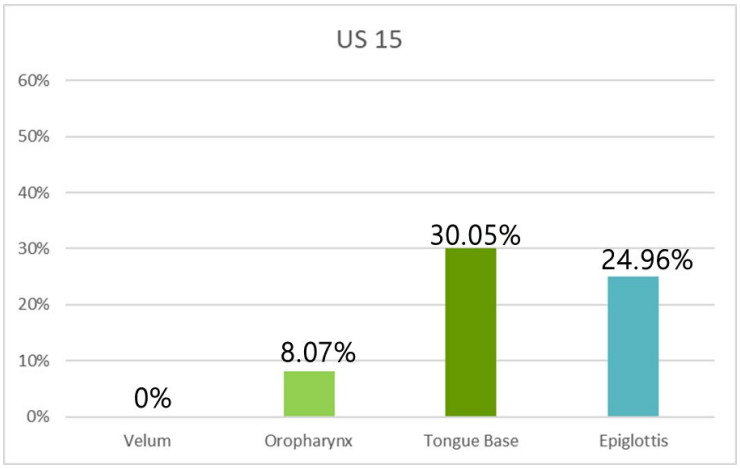
DocuSign Envelope ID: FF917FA4-BEA0-4E08-96D0-A9016C337F14

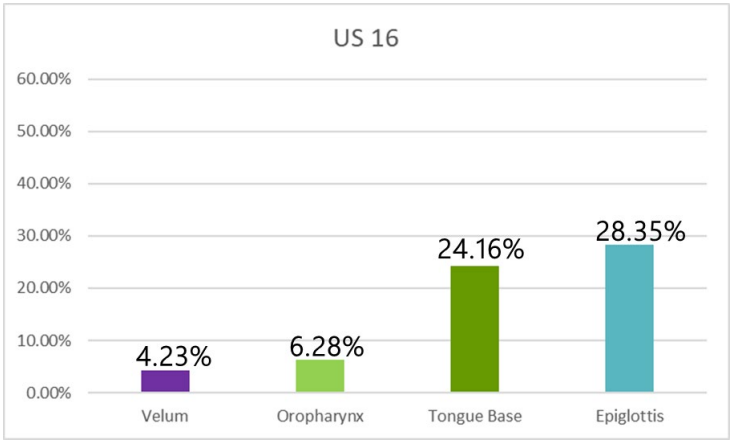


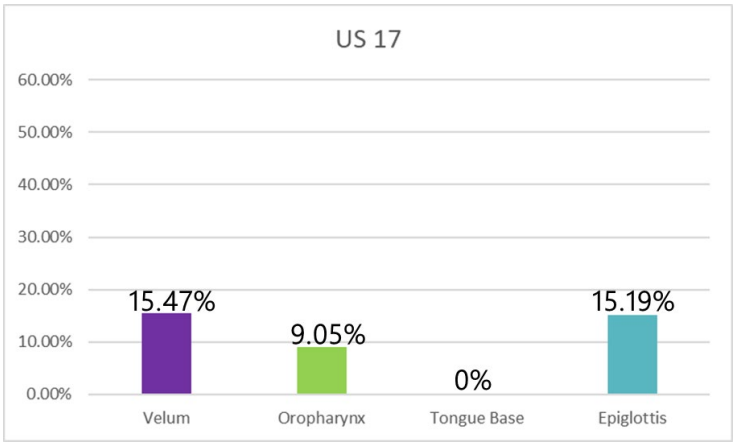




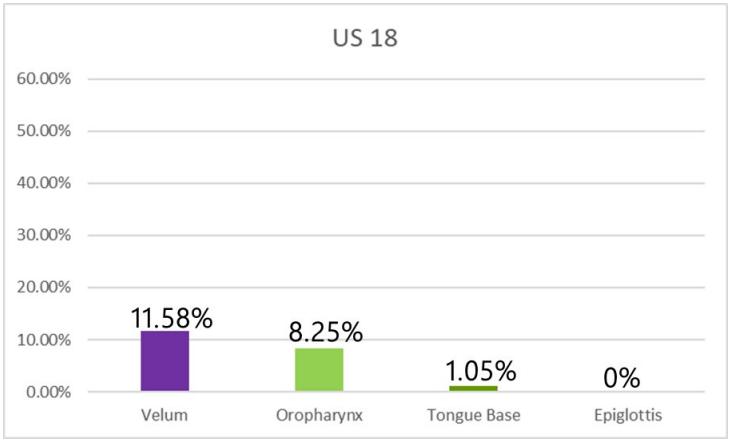
DocuSign Envelope ID: FF917FA4-BEA0-4E08-96D0-A9016C337F14







DocuSign Envelope ID: FF917FA4-BEA0-4E08-96D0-A9016C337F14



DocuSign Envelope ID: FF917FA4-BEA0-4E08-96D0-A9016C337F14

Appendix E: Airspace Contraction (Collapse) Raw Data Per Subject

US 1 Raw Data	Normal_1	Normal_2	Normal_3	Muller_1	Muller_2	Muller_3
Width.V.Max	3.536	3.796	3.203	2.665	3.367	3.195
Width.V.P75	3.505	3.607	2.573	2.59	3.271	2.266
Width.V.Mean	3.266045455	3.179177778	2.427347826	1.817431818	2.760795455	1.806021739
Width.V.P25	3.152	2.685	2.353	1.172	2.432	1.299
Width.V.Min	2.409	1.747	1.08	1	1.256	0.969
Width.V.Median	3.448	3.397	2.51	2.144	3.243	1.363
Width.O.Max	2.952	3.882	3.085	3.016	2.905	3.156
Width.O.P75	2.89	2.841	2.432	2.859	2.81	3.084
Width.O.Mean	2.437681818	2.501911111	2.389695652	2.447744186	2.628045455	2.939956522
Width.O.P25	2.114	2.223	2.196	1.873	2.429	2.828
Width.O.Min	1.842	1.315	2.06	1.657	2.222	2.414
Width.O.Median	2.225	2.448	2.353	2.718	2.716	3.032
Width.T.Max	3.534	4.212	3.46	3.373	3.262	3.135
Width.T.P75	3.484	3.857	3.13	3.11	3.185	3.064
Width.T.Mean	3.126295455	3.397844444	2.994217391	2.857116279	3.113613636	2.94426087
Width.T.P25	2.922	3.066	2.829	2.821	3.066	2.859
Width.T.Min	2.808	2.889	2.651	1.778	2.937	2.705
Width.T.Median	2.984	3.213	3.042	2.98	3.112	2.944
Width.E.Max	3.242	2.991	3.27	3.088	3.356	2.842
Width.E.P75	3.187	2.897	3.169	2.88	3.335	2.704
Width.E.Mean	2.977767442	2.875377778	2.999630435	2.793139535	3.265295455	2.662933333
Width.E.P25	2.857	2.858	2.853	2.693	3.274	2.621
Width.E.Min	2.766	2.737	2.757	2.657	2.771	2.417
Width.E.Median	2.894	2.878	2.914	2.743	3.292	2.67

DocuSign Envelope ID: FF917FA4-BEA0-4E08-96D0-A9016C337F14

US 2 Raw Data	Normal_1	Normal_2	Normal_3	Muller_1	Muller_2	Muller_3
Width.V.Max	4.333	4.302	4.564	4.148	3.67	3.561
Width.V.P75	3.985	4.27	4.54	4.065	3.609	3.127
Width.V.Mean	3.704891304	3.921979167	4.396416667	3.78976087	3.371333333	3.068851064
Width.V.P25	3.468	3.692	4.353	3.429	3.273	2.959
Width.V.Min	2.748	3.361	4.074	3.239	1.687	2.77
Width.V.Median	3.587	3.832	4.428	3.93	3.531	3.087
Width.O.Max	4.307	4.281	4.472	3.651	3.29	3.386
Width.O.P75	3.755	4.151	4.389	3.561	3.175	3.325
Width.O.Mean	3.732217391	3.728191489	4.249829787	3.441333333	2.70912766	3.241851064
Width.O.P25	3.54	3.334	4.142	3.35	2.382	3.205
Width.O.Min	3.415	2.889	3.922	3.197	1.321	2.621
Width.O.Median	3.724	3.872	4.259	3.459	2.816	3.271
Width.T.Max	4.663	3.619	4.083	3.074	2.088	3.013
Width.T.P75	4.552	3.524	3.816	2.229	1.853	2.758
Width.T.Mean	4.152826087	3.230729167	3.556255319	2.011	1.747229167	2.436297872
Width.T.P25	3.774	3.087	3.35	1.704	1.583	2.199
Width.T.Min	3.383	2.702	2.753	1.602	1.453	1.295
Width.T.Median	4.324	3.26	3.666	1.891	1.754	2.503
Width.E.Max	1.751	1.644	2.304	1.612	3.081	2.416
Width.E.P75	1.616	1.556	1.721	1.315	2.372	2.081
Width.E.Mean	1.528043478	1.493148936	1.623468085	1.159066667	2.281744681	1.612297872
Width.E.P25	1.46	1.466	1.4	1.013	2.109	1.382
Width.E.Min	1.248	1.099	1.256	0.753	1.767	0.892
Width.E.Median	1.526	1.498	1.601	1.154	2.308	1.467

DocuSign Envelope ID: FF917FA4-BEA0-4E08-96D0-A9016C337F14

US 3 Raw Data	Normal_1	Normal_2	Normal_3	Muller_1	Muller_2	Muller_3
Width.V.Max	4.27	4.493	4.532	4.188	4.036	4.437
Width.V.P75	3.985	4.305	4.515	3.875	3.999	3.99
Width.V.Mean	3.882	4.049489362	4.436043478	3.841489362	3.883765957	3.847468085
Width.V.P25	3.787	3.863	4.332	3.73	3.763	3.667
Width.V.Min	3.73	3.834	4.27	3.714	3.381	3.619
Width.V.Median	3.807	3.914	4.483	3.779	3.944	3.769
Width.O.Max	4.27	4.353	4.099	4.254	3.722	4.07
Width.O.P75	4.191	3.889	3.937	4.178	3.695	3.971
Width.O.Mean	3.838042553	3.565808511	3.542422222	4.002934783	3.609446809	3.477217391
Width.O.P25	3.603	2.95	3.291	4.003	3.685	2.75
Width.O.Min	2.871	2.705	2.728	2.82	2.619	2.305
Width.O.Median	4.032	3.841	3.45	4.13	3.69	3.877
Width.T.Max	3.731	3.382	3.538	3.41	3.438	3.335
Width.T.P75	3.541	3.168	3.415	3.331	3.162	3.19
Width.T.Mean	3.291914894	3.093276596	3.219282609	3.197723404	3.126319149	3.12306383
Width.T.P25	3.081	3.017	3.032	3.113	3.051	3.057
Width.T.Min	2.86	2.688	2.863	2.738	2.899	2.923
Width.T.Median	3.335	3.082	3.165	3.247	3.087	3.111
Width.E.Max	3.35	3.245	3.207	3.653	3.206	3.158
Width.E.P75	3.271	3.188	3.152	3.382	2.955	3.079
Width.E.Mean	3.191434783	3.145652174	3.0666	3.286326087	2.896085106	2.999304348
Width.E.P25	3.066	3.107	2.973	3.182	2.815	2.939
Width.E.Min	2.941	3.038	2.813	2.872	2.481	2.775
Width.E.Median	3.27	3.152	3.103	3.31	2.892	3.039

DocuSign Envelope ID: FF917FA4-BEA0-4E08-96D0-A9016C337F14

US 4 Raw Data	Normal_1	Normal_2	Normal_3	Muller_1	Muller_2	Muller_3
Width.V.Max	4.554	4.089	3.802	4.289	4.039	4.056
Width.V.P75	4.412	3.885	3.592	4.176	3.843	3.851
Width.V.Mean	4.322173913	3.868191489	3.559765957	3.780446809	3.618829787	3.723404255
Width.V.P25	4.217	3.854	3.478	3.287	3.409	3.631
Width.V.Min	4.094	3.437	3.43	3.167	3.298	3.222
Width.V.Median	4.328	3.88	3.543	3.943	3.556	3.787
Width.O.Max	4.011	4.168	3.643	3.21	3.844	3.646
Width.O.P75	3.907	3.951	3.419	3.178	3.601	3.244
Width.O.Mean	3.760911111	3.727489362	3.372361702	3.019586957	3.417456522	3.122851064
Width.O.P25	3.615	3.55	3.292	2.9	3.292	2.932
Width.O.Min	3.542	3.28	3.049	2.503	2.03	2.779
Width.O.Median	3.746	3.674	3.343	3.108	3.428	3.163
Width.T.Max	3.615	3.515	3.537	3.026	3.469	3.935
Width.T.P75	3.387	3.282	2.859	2.496	2.644	3.615
Width.T.Mean	3.026652174	2.764574468	2.533659574	2.37487234	2.38587234	3.136680851
Width.T.P25	2.88	2.245	2.028	2.19	2.025	2.793
Width.T.Min	2.028	1.908	1.857	1.477	1.386	2.244
Width.T.Median	3.132	3.048	2.415	2.318	2.422	3.149
Width.E.Max	2.725	2.93	4.25	3.154	3.381	4.268
Width.E.P75	2.066	2.849	4.183	2.852	2.239	4.191
Width.E.Mean	2.069288889	2.718108696	3.644108696	2.494	1.903282609	4.006652174
Width.E.P25	1.939	2.668	3.394	2.222	1.399	3.988
Width.E.Min	1.794	2.035	1.79	1.906	1.095	2.92
Width.E.Median	2	2.831	3.89	2.373	1.707	4.05

DocuSign Envelope ID: FF917FA4-BEA0-4E08-96D0-A9016C337F14

US 5 Raw Data	Normal_1	Normal_2	Normal_3	Muller_1	Muller_2	Muller_3
Width.V.Max	4.556	5.569	5.151	5.007	5.05	5.371
Width.V.P75	4.507	5.522	5.09	4.973	4.985	5.324
Width.V.Mean	4.443	5.113297872	5.0136875	4.628787234	4.831510638	5.228914894
Width.V.P25	4.386	4.906	4.96	4.196	4.689	5.102
Width.V.Min	4.321	4.734	4.926	3.96	4.498	4.942
Width.V.Median	4.452	4.943	4.993	4.71	4.869	5.263
Width.O.Max	4.357	4.543	4.811	4.064	4.183	4.716
Width.O.P75	4.244	4.334	4.75	3.607	3.85	4.35
Width.O.Mean	3.785244444	4.255510638	4.497957447	3.466106383	3.658021277	4.021297872
Width.O.P25	3.35	4.177	4.259	3.35	3.397	3.701
Width.O.Min	2.906	3.718	4.016	2.683	3.179	3.418
Width.O.Median	3.672	4.286	4.606	3.466	3.671	3.902
Width.T.Max	4.046	4.286	4.436	3.682	3.623	3.173
Width.T.P75	3.816	4.111	4.254	3.302	3.286	3.064
Width.T.Mean	3.519782609	3.912425532	4.027914894	3.056723404	2.982808511	2.847531915
Width.T.P25	3.336	3.759	3.84	2.622	2.672	2.685
Width.T.Min	2.977	3.373	3.354	2.318	2.476	2.526
Width.T.Median	3.466	3.879	4.103	3.127	3.003	2.863
Width.E.Max	3.47	4.357	4.461	4.375	3.737	3.159
Width.E.P75	3.317	4.245	4.306	4.274	3.658	3.127
Width.E.Mean	2.874777778	4.049804348	3.852170213	3.469319149	3.503446809	2.822361702
Width.E.P25	3.06	3.881	3.623	3.073	3.511	2.587
Width.E.Min	1.48	3.798	3.595	2.747	2.87	2.48
Width.E.Median	3.271	4.043	3.672	3.21	3.56	2.778

DocuSign Envelope ID: FF917FA4-BEA0-4E08-96D0-A9016C337F14

US 6 Raw Data	Normal_1	Normal_2	Normal_3	Muller_1	Muller_2	Muller_3
Width.V.Max	5.732	6.025	5.695	5.335	5.357	5.318
Width.V.P75	5.264	5.715	5.252	4.987	4.978	5.079
Width.V.Mean	5.184804348	5.510042553	5.206854167	4.733914894	4.811085106	4.925916667
Width.V.P25	5.074	5.394	5.113	4.346	4.714	4.826
Width.V.Min	4.876	4.953	4.96	4.209	4.115	4.149
Width.V.Median	5.156	5.439	5.206	4.798	4.796	5.048
Width.O.Max	5.824	6.383	6.035	5.778	5.747	5.049
Width.O.P75	5.651	6.041	5.841	5.605	5.5	3.69
Width.O.Mean	5.600577778	5.956553191	5.395404255	5.150148936	5.227468085	3.469340426
Width.O.P25	5.556	5.852	5.257	4.73	4.922	3.021
Width.O.Min	5.365	5.626	4.285	4.198	4.664	2.461
Width.O.Median	5.619	5.915	5.461	5.307	5.208	3.39
Width.T.Max	5.422	5.874	5.955	4.55	5.048	4.252
Width.T.P75	5.275	5.77	5.809	4.167	4.778	4.081
Width.T.Mean	4.341173913	5.181212766	5.617978723	3.916297872	4.216595745	3.344808511
Width.T.P25	3.484	4.622	5.529	3.748	3.334	2.867
Width.T.Min	3.08	3.508	4.955	3.335	3.112	2.113
Width.T.Median	4.175	5.422	5.588	3.858	4.677	3.242
Width.E.Max	3.546	4.413	5.134	4.048	3.893	4.267
Width.E.P75	3.406	4.08	4.041	3.873	3.625	3.162
Width.E.Mean	3.238333333	3.913531915	3.979404255	3.755744681	3.550659574	2.869085106
Width.E.P25	3.083	3.748	3.672	3.695	3.55	2.551
Width.E.Min	2.842	3.514	3.539	3.288	2.671	1.73
Width.E.Median	3.248	3.937	3.783	3.775	3.582	2.843

DocuSign Envelope ID: FF917FA4-BEA0-4E08-96D0-A9016C337F14

US 7 Raw Data	Normal_1	Normal_2	Normal_3	Muller_1	Muller_2	Muller_3
Width.V.Max	4.125	4.334	3.139	3.28	3.29	3.939
Width.V.P75	3.79	4.058	3.107	3.086	2.955	3.365
Width.V.Mean	3.725808511	3.738319149	2.899787234	2.980829787	2.920723404	3.166298
Width.V.P25	3.667	3.282	2.63	2.859	2.86	3.017
Width.V.Min	3.146	3.017	2.222	2.754	2.588	2.706
Width.V.Median	3.743	3.993	3.021	2.957	2.923	3.053
Width.O.Max	4.278	4.162	4.035	3.319	2.968	3.032
Width.O.P75	3.826	3.985	3.568	2.764	2.394	2.446
Width.O.Mean	3.712042553	3.489404255	3.407468085	2.682340426	2.324787234	2.269851
Width.O.P25	3.562	3.076	3.222	2.54	2.151	2.065
Width.O.Min	3.051	2.775	2.779	2.114	2.052	1.886
Width.O.Median	3.699	3.4	3.365	2.699	2.292	2.216
Width.T.Max	3.466	4.347	3.583	3.593	3.219	2.426
Width.T.P75	3.263	3.795	3.413	2.715	3.083	2.278
Width.T.Mean	3.226021277	3.664468085	3.157744681	2.62512766	2.970297872	2.193957
Width.T.P25	3.172	3.578	3.032	2.444	2.896	2.098
Width.T.Min	3.068	3.226	1.921	1.305	2.32	1.963
Width.T.Median	3.215	3.695	3.128	2.651	3.003	2.184
Width.E.Max	3.755	3.507	3.816	2.842	2.942	2.988
Width.E.P75	3.437	3.318	3.615	2.314	2.892	2.892
Width.E.Mean	3.365152174	2.592565217	3.326106383	2.03612766	2.791652174	2.741319
Width.E.P25	3.282	2.198	3.085	1.731	2.719	2.794
Width.E.Min	3.048	1.068	2.875	0.731	2.51	1.895
Width.E.Median	3.375	2.619	3.223	2.108	2.835	2.851

DocuSign Envelope ID: FF917FA4-BEA0-4E08-96D0-A9016C337F14

US 8 Raw Data	Normal_1	Normal_2	Normal_3	Muller_1	Muller_2	Muller_3
Width.V.Max	4.381	5.256	4.402	4.588	4.794	4.3
Width.V.P75	4.099	4.971	4.303	4.398	4.66	4.064
Width.V.Mean	4.085804348	4.901276596	3.682145833	4.354574468	4.298404255	3.876083333
Width.V.P25	4.034	4.862	3.173	4.318	3.968	3.606
Width.V.Min	4.003	3.971	3.027	4.1	3.261	3.527
Width.V.Median	4.051	4.953	3.387	4.344	4.626	3.977
Width.O.Max	4.862	4.8	3.908	3.34	3.651	3.954
Width.O.P75	4.479	4.689	3.73	3.334	2.995	3.724
Width.O.Mean	4.000108696	4.329531915	3.370829787	2.707531915	2.882638298	3.408744681
Width.O.P25	3.399	4.191	3.113	2.397	2.654	3.128
Width.O.Min	3.251	3.29	2.719	2.113	2.459	2.698
Width.O.Median	4.222	4.328	3.235	2.475	2.944	3.494
Width.T.Max	3.399	3.231	3.366	3.053	3.089	3.081
Width.T.P75	3.176	3.068	3.146	2.783	2.923	3.002
Width.T.Mean	3.128173913	2.966744681	3.0124375	2.592957447	2.700148936	2.7863125
Width.T.P25	3.053	2.848	2.89	2.384	2.462	2.624
Width.T.Min	2.952	2.604	2.75	2.218	2.099	2.447
Width.T.Median	3.119	2.998	3.001	2.538	2.607	2.806
Width.E.Max	3.213	3.509	3.049	2.422	2.736	3.06
Width.E.P75	2.926	3.454	2.854	2.218	2.641	2.934
Width.E.Mean	2.917369565	3.27623913	2.774744681	1.859574468	2.518043478	2.700170213
Width.E.P25	2.867	3.085	2.722	1.545	2.478	2.449
Width.E.Min	2.779	2.899	2.53	0.27	2.039	2.369
Width.E.Median	2.896	3.329	2.756	2.16	2.546	2.773

DocuSign Envelope ID: FF917FA4-BEA0-4E08-96D0-A9016C337F14

US 9 Raw Data	Normal_1	Normal_2	Normal_3	Muller_1	Muller_2	Muller_3
Width.V.Max	1.782	1.669	1.647	1.433	1.574	1.555
Width.V.P75	1.626	1.398	1.601	1.165	1.54	1.386
Width.V.Mean	1.502891304	1.261702128	1.566645833	1.124782609	1.408958333	1.324319149
Width.V.P25	1.415	1.043	1.551	1.038	1.445	1.239
Width.V.Min	0.889	0.798	1.398	0.875	0.938	1.176
Width.V.Median	1.536	1.364	1.581	1.08	1.508	1.334
Width.O.Max	1.37	1.524	1.42	2.376	1.414	2.043
Width.O.P75	1.215	1.271	1.286	2.258	1.324	1.207
Width.O.Mean	1.160326087	1.203382979	1.173106383	1.858086957	1.104680851	1.233744681
Width.O.P25	1.082	1.143	1.066	1.713	0.937	1.086
Width.O.Min	1.002	1.008	0.857	1.064	0.763	0.953
Width.O.Median	1.147	1.177	1.146	1.841	1.055	1.154
Width.T.Max	1.964	3.816	4.931	3.682	3.412	2.273
Width.T.P75	1.865	3.748	4.667	3.415	3.288	2.165
Width.T.Mean	1.39026087	3.476446809	4.461702128	2.7755	3.2090625	1.800042553
Width.T.P25	1.15	3.186	4.397	2.281	3.119	1.421
Width.T.Min	0.903	2.295	2.691	1.171	3.06	1.219
Width.T.Median	1.181	3.652	4.525	2.88	3.188	1.823
Width.E.Max	3.344	4.958	5.463	3.78	3.123	4.097
Width.E.P75	2.873	4.909	5.076	2.953	3.066	3.738
Width.E.Mean	2.556933333	4.716361702	4.899382979	2.28976087	1.927297872	3.508702128
Width.E.P25	2.399	4.796	4.747	1.703	1.051	3.409
Width.E.Min	1.767	3.108	4.4	0.92	0.804	2.068
Width.E.Median	2.47	4.863	4.766	2.329	1.78	3.595

DocuSign Envelope ID: FF917FA4-BEA0-4E08-96D0-A9016C337F14

US 10 Raw Data	Normal_1	Normal_2	Normal_3	Muller_1	Muller_2	Muller_3
Width.V.Max	4.366	3.85	4.271	3.572	4.241	4.066
Width.V.P75	4.056	3.812	4.163	3.516	4.043	3.813
Width.V.Mean	4.014145833	3.778893617	4.067468085	3.404195652	3.878553191	3.743744681
Width.V.P25	3.953	3.794	3.939	3.302	3.691	3.642
Width.V.Min	3.739	3.429	3.812	3.066	3.603	3.492
Width.V.Median	3.99	3.798	4.1	3.479	3.817	3.688
Width.O.Max	4.1	4.498	4.009	3.271	3.699	3.286
Width.O.P75	4.021	4.356	3.961	3.048	3.365	3.128
Width.O.Mean	3.962541667	4.099893617	3.803319149	2.895222222	3.199531915	2.974108696
Width.O.P25	3.927	3.913	3.659	2.723	2.971	2.795
Width.O.Min	3.794	3.794	3.402	2.635	2.826	2.619
Width.O.Median	3.961	4.038	3.898	2.894	3.16	3.032
Width.T.Max	3.932	3.759	3.429	2.508	2.954	2.986
Width.T.P75	3.885	3.487	3.303	2.334	2.784	2.829
Width.T.Mean	3.795708333	3.397382979	3.173170213	2.172777778	2.563382979	2.510404255
Width.T.P25	3.741	3.34	3.005	1.995	2.287	2.244
Width.T.Min	3.576	3.097	2.985	1.814	2.222	2.196
Width.T.Median	3.807	3.399	3.194	2.206	2.603	2.397
Width.E.Max	3.578	3.825	3.857	2.767	3.561	3.243
Width.E.P75	3.38	3.509	3.309	2.254	3.027	3.004
Width.E.Mean	3.218425532	3.374765957	3.184531915	2.225022222	3.00526087	2.813913043
Width.E.P25	3.085	3.213	3.032	2.095	2.923	2.83
Width.E.Min	3.052	2.925	2.254	1.907	2.878	1.812
Width.E.Median	3.115	3.431	3.246	2.176	2.982	2.87

DocuSign Envelope ID: FF917FA4-BEA0-4E08-96D0-A9016C337F14

US 11 Raw Data	Normal_1	Normal_2	Normal_3	Muller_1	Muller_2	Muller_3
Width.V.Max	4.615	4.612	4.347	4.265	4.274	3.607
Width.V.P75	4.6	4.556	3.703	4.166	4.259	3.526
Width.V.Mean	4.573416667	4.308145833	3.6029375	3.952270833	4.1104375	3.488895833
Width.V.P25	4.556	4.113	3.461	3.588	4.07	3.462
Width.V.Min	4.494	4.013	2.764	3.544	3.572	3.303
Width.V.Median	4.587	4.144	3.672	4.133	4.227	3.51
Width.O.Max	4.464	4.255	3.438	3.607	3.814	3.429
Width.O.P75	4.446	3.658	2.858	3.573	3.543	3.286
Width.O.Mean	4.151404255	3.639489362	2.680170213	3.126531915	2.998	3.122510638
Width.O.P25	3.883	3.493	2.406	2.875	2.398	2.923
Width.O.Min	3.562	3.214	2.254	2.384	2.287	2.68
Width.O.Median	4.249	3.596	2.548	3.207	3.002	3.164
Width.T.Max	3.672	4.171	4.193	2.858	3.392	3.318
Width.T.P75	3.549	3.444	3.564	2.826	3.241	3.144
Width.T.Mean	3.320702128	2.942382979	3.101791667	2.574021277	2.932833333	2.989595745
Width.T.P25	3.346	2.534	2.905	2.397	2.652	2.907
Width.T.Min	2.572	2.111	2.238	2.334	2.389	2.532
Width.T.Median	3.446	2.858	3.049	2.495	2.889	3.002
Width.E.Max	2.832	2.973	3.049	2.858	2.734	3.174
Width.E.P75	2.719	2.93	3.017	2.702	2.62	3.156
Width.E.Mean	2.623702128	2.58087234	2.665638298	2.529914894	2.575957447	2.971829787
Width.E.P25	2.524	2.222	2.261	2.27	2.501	3.029
Width.E.Min	2.406	2.053	1.971	2.143	2.367	2.003
Width.E.Median	2.606	2.73	2.858	2.686	2.575	3.105

DocuSign Envelope ID: FF917FA4-BEA0-4E08-96D0-A9016C337F14

US 12 Raw Data	Normal_1	Normal_2	Normal_3	Muller_1	Muller_2	Muller_3
Width.V.Max	3.494	3.205	3.947	3.135	3.271	3.145
Width.V.P75	3.431	3.189	3.32	3.104	3.19	3.128
Width.V.Mean	3.219695652	2.926479167	3.295291667	2.854021277	2.811958333	2.970125
Width.V.P25	3.143	2.984	3.256	2.614	2.779	2.99
Width.V.Min	2.245	1.016	2.874	0.932	1.423	2.159
Width.V.Median	3.356	3.115	3.272	3.017	3.143	3.127
Width.O.Max	3.225	3.238	3.209	2.771	2.891	3.615
Width.O.P75	3.022	3.019	2.635	2.747	2.686	3.509
Width.O.Mean	2.829155556	2.858979167	2.366702128	1.995021739	2.412166667	2.846458333
Width.O.P25	2.783	2.937	2.002	1.438	2.247	2.543
Width.O.Min	1.76	1.444	1.607	0.857	1.603	1.916
Width.O.Median	2.912	2.985	2.389	2.023	2.513	2.75
Width.T.Max	3.07	3	2.953	3.177	3.064	2.758
Width.T.P75	2.985	2.921	2.905	3.098	2.825	2.63
Width.T.Mean	2.9244	2.853645833	2.851708333	3.008893617	2.577166667	2.437791667
Width.T.P25	2.857	2.826	2.83	2.923	2.477	2.27
Width.T.Min	2.762	2.635	2.527	2.736	1.475	1.051
Width.T.Median	2.937	2.874	2.874	3.047	2.698	2.572
Width.E.Max	3.35	3.354	2.898	3.018	2.677	3.056
Width.E.P75	3.301	3.22	2.772	2.86	2.573	3.028
Width.E.Mean	3.221666667	3.100510638	2.557957447	2.744891304	2.395659574	2.8033125
Width.E.P25	3.165	2.986	2.381	2.672	2.239	2.699
Width.E.Min	2.921	2.73	2.108	2.263	2.066	2.299
Width.E.Median	3.264	3.131	2.579	2.81	2.36	2.769

DocuSign Envelope ID: FF917FA4-BEA0-4E08-96D0-A9016C337F14

US 13 Raw Data	Normal_1	Normal_2	Normal_3	Muller_1	Muller_2	Muller_3
Width.V.Max	4.472	3.942	5.207	4.626	4.564	4.197
Width.V.P75	4.365	3.699	4.774	4.535	4.52	4.104
Width.V.Mean	4.188645833	3.671041667	4.711833333	4.3816875	4.076979167	3.978770833
Width.V.P25	4.1	3.619	4.658	4.311	3.914	3.909
Width.V.Min	4.064	3.573	4.489	3.755	3.854	3.565
Width.V.Median	4.131	3.667	4.701	4.437	3.942	4.039
Width.O.Max	5.223	4.411	4.67	5.206	4.079	3.683
Width.O.P75	5.06	4.231	4.084	5.119	3.82	3.056
Width.O.Mean	4.470276596	3.91893617	3.944340426	4.728212766	3.586829787	2.881255319
Width.O.P25	3.849	3.81	3.746	4.477	3.461	2.684
Width.O.Min	3.402	2.839	3.651	3.365	2.206	2.233
Width.O.Median	4.521	4.003	3.896	4.597	3.641	2.75
Width.T.Max	4.016	4.104	4.217	3.222	3.404	2.889
Width.T.P75	3.831	3.731	4.111	2.684	3.159	2.779
Width.T.Mean	3.600625	3.627276596	3.868659574	2.525808511	2.671958333	2.589085106
Width.T.P25	3.384	3.559	3.587	2.272	2.402	2.462
Width.T.Min	3.161	3.245	3.343	2.131	2.208	2.159
Width.T.Median	3.672	3.626	3.968	2.485	2.503	2.62
Width.E.Max	3.998	3.839	3.931	4.001	3.282	2.365
Width.E.P75	3.88	3.712	3.863	3.921	3.199	2.143
Width.E.Mean	3.691404255	3.498957447	3.790489362	3.694404255	2.800489362	1.953851064
Width.E.P25	3.625	3.322	3.69	3.518	2.319	1.794
Width.E.Min	3.07	3.096	3.625	2.868	2.161	1.607
Width.E.Median	3.764	3.478	3.812	3.715	3.102	1.911

DocuSign Envelope ID: FF917FA4-BEA0-4E08-96D0-A9016C337F14

US 14 Raw Data	Normal_1	Normal_2	Normal_3	Muller_1	Muller_2	Muller_3
Width.V.Max	2.971	4.102	3.59	2.804	3.731	2.049
Width.V.P75	2.941	4.038	2.033	2.623	3.143	1.944
Width.V.Mean	2.924978723	3.38706383	2.271234043	2.299723404	3.139916667	1.922234043
Width.V.P25	2.922	2.735	1.999	2.056	3.115	1.898
Width.V.Min	2.812	2.16	1.949	1.335	3.085	1.81
Width.V.Median	2.939	3.77	2.013	2.284	3.131	1.928
Width.O.Max	3.527	3.628	3.594	2.75	3.172	2.071
Width.O.P75	3.298	3.494	3.465	2.525	2.926	1.969
Width.O.Mean	3.181782609	3.287510638	3.084489362	2.238148936	2.906170213	1.851234043
Width.O.P25	3.032	3.107	2.69	1.971	2.853	1.72
Width.O.Min	2.854	2.821	2.437	1.667	2.837	1.596
Width.O.Median	3.225	3.302	3.098	2.176	2.873	1.853
Width.T.Max	3.318	3.384	3.141	3.561	2.715	3.226
Width.T.P75	3.227	3.112	2.932	3.555	1.953	3.194
Width.T.Mean	3.164617021	2.849851064	2.652255319	3.363191489	1.65306383	2.54712766
Width.T.P25	3.127	2.508	2.59	3.142	1.32	1.323
Width.T.Min	2.913	1.94	1.36	3.032	0.853	1.14
Width.T.Median	3.197	2.93	2.763	3.388	1.463	3.066
Width.E.Max	3.211	1.981	2.529	3.487	2.367	2.702
Width.E.P75	3.119	1.924	1.937	2.936	2.101	1.867
Width.E.Mean	2.932391304	1.810893617	1.625829787	2.849608696	1.789212766	1.588765957
Width.E.P25	2.915	1.762	1.398	2.638	1.509	1.152
Width.E.Min	2.299	1.182	0.608	2.584	1.396	0.801
Width.E.Median	2.972	1.842	1.621	2.784	1.697	1.471

DocuSign Envelope ID: FF917FA4-BEA0-4E08-96D0-A9016C337F14

US 15 Raw Data	Normal_1	Normal_2	Normal_3	Muller_1	Muller_2	Muller_3
Width.V.Max	3.538	3.159	3.028	3.038	3.246	3.386
Width.V.P75	3.044	2.796	2.97	2.905	2.995	2.969
Width.V.Mean	2.792914894	2.759361702	2.787893617	2.719595745	2.813416667	2.74987234
Width.V.P25	2.481	2.641	2.609	2.617	2.542	2.429
Width.V.Min	1.887	2.595	2.224	2.115	2.082	1.963
Width.V.Median	2.853	2.681	2.876	2.81	2.907	2.874
Width.O.Max	3.641	3.445	3.079	3.932	2.862	2.853
Width.O.P75	3.433	2.881	2.812	3.111	2.606	2.418
Width.O.Mean	2.812617021	2.844391304	2.667829787	2.707217391	2.375361702	2.318914894
Width.O.P25	2.335	2.721	2.545	2.455	2.169	2.222
Width.O.Min	1.994	2.624	2.245	2.054	1.81	1.876
Width.O.Median	2.522	2.821	2.626	2.631	2.414	2.327
Width.T.Max	3.048	3.592	2.847	2.54	3.066	2.781
Width.T.P75	2.807	3.523	2.68	2.191	2.619	2.636
Width.T.Mean	2.762595745	3.218304348	2.505744681	1.937021739	2.136234043	2.171382979
Width.T.P25	2.621	3.111	2.302	1.683	1.729	1.627
Width.T.Min	2.45	2.81	2.175	1.512	1.585	1.477
Width.T.Median	2.772	3.155	2.568	1.939	1.879	2.256
Width.E.Max	2.258	3.038	3.422	2.996	2.345	3.903
Width.E.P75	1.824	2.815	3.164	2.143	1.942	3.31
Width.E.Mean	1.818531915	2.639326087	2.867297872	2.006934783	1.850297872	2.751425532
Width.E.P25	1.795	2.379	2.643	1.502	1.719	2.257
Width.E.Min	1.78	2.188	2.429	1.446	1.613	2.064
Width.E.Median	1.809	2.764	2.833	2.074	1.867	2.525

DocuSign Envelope ID: FF917FA4-BEA0-4E08-96D0-A9016C337F14

US 16 Raw Data	Normal_1	Normal_2	Normal_3	Muller_1	Muller_2	Muller_3
Width.V.Max	4.35	2.791	3.103	3.149	3.017	2.969
Width.V.P75	3.683	2.51	2.99	3.032	2.8	2.894
Width.V.Mean	3.604416667	2.320191489	2.810744681	2.940782609	2.778787234	2.779468085
Width.V.P25	3.542	2.258	2.651	2.909	2.731	2.706
Width.V.Min	3.074	1.325	2.179	2.349	2.559	2.572
Width.V.Median	3.612	2.294	2.905	2.984	2.778	2.782
Width.O.Max	3.311	2.423	2.858	3.067	3.011	3.129
Width.O.P75	3.042	2.379	2.719	2.802	2.865	2.588
Width.O.Mean	2.48793617	2.102808511	2.394212766	2.581152174	2.561446809	2.128586957
Width.O.P25	1.727	1.906	2.008	2.349	2.273	1.664
Width.O.Min	0.994	1.186	0.99	2.196	2.067	1.048
Width.O.Median	2.77	2.135	2.645	2.479	2.526	2.112
Width.T.Max	2.447	2.308	2.393	2.675	1.866	1.715
Width.T.P75	2.4	2.113	2.112	2.465	1.679	1.453
Width.T.Mean	2.2754375	2.00106383	1.974340426	2.152586957	1.525297872	1.343255319
Width.T.P25	2.338	1.906	1.803	1.903	1.428	1.207
Width.T.Min	1.651	1.762	1.692	1.577	1.127	0.874
Width.T.Median	2.384	2.016	1.906	2.101	1.529	1.397
Width.E.Max	2.616	2.795	2.59	2.283	2.558	1.794
Width.E.P75	2.545	2.763	2.559	2.075	2.264	1.541
Width.E.Mean	2.530638298	2.68226087	2.247170213	1.82876087	2.059829787	1.479826087
Width.E.P25	2.512	2.605	1.946	1.56	1.858	1.407
Width.E.Min	2.48	2.461	1.76	1.29	1.62	1.304
Width.E.Median	2.529	2.717	2.435	1.812	1.954	1.479

DocuSign Envelope ID: FF917FA4-BEA0-4E08-96D0-A9016C337F14

US 17 Raw Data	Normal_1	Normal_2	Normal_3	Muller_1	Muller_2	Muller_3
Width.V.Max	4.419	5.919	5.715	4.921	5.538	4.937
Width.V.P75	4.346	5.815	5.694	4.822	5.168	4.81
Width.V.Mean	4.331829787	5.6545625	5.597895833	4.641020833	5.116553191	4.687208333
Width.V.P25	4.314	5.559	5.556	4.481	5.017	4.578
Width.V.Min	4.243	4.876	5.315	4.382	4.953	4.416
Width.V.Median	4.33	5.784	5.656	4.638	5.065	4.685
Width.O.Max	5.498	4.71	5.351	4.711	4.684	4.621
Width.O.P75	5.175	4.431	5.111	4.544	4.635	4.462
Width.O.Mean	4.751108696	4.366255319	4.627914894	4.501021277	4.441212766	4.425833333
Width.O.P25	4.444	4.307	4.338	4.418	4.344	4.393
Width.O.Min	4.345	4.233	4.227	4.354	4.206	4.27
Width.O.Median	4.605	4.333	4.418	4.477	4.384	4.433
Width.T.Max	5.154	4.952	4.408	4.702	4.353	4.806
Width.T.P75	4.893	4.694	4.255	4.601	4.31	4.67
Width.T.Mean	4.749804348	4.313531915	4.12725	4.505382979	4.25806383	4.471583333
Width.T.P25	4.587	4.063	3.972	4.401	4.211	4.286
Width.T.Min	4.388	3.921	3.827	4.114	4.067	4.1
Width.T.Median	4.831	4.175	4.162	4.529	4.287	4.485
Width.E.Max	4.497	3.689	3.973	4.464	4.387	4.237
Width.E.P75	4.429	3.643	3.938	4.195	4.262	4.053
Width.E.Mean	3.419304348	3.593468085	3.838361702	3.977297872	3.930723404	3.895340426
Width.E.P25	2.876	3.56	3.729	3.735	3.767	3.636
Width.E.Min	2.779	3.44	3.58	3.648	3.604	3.603
Width.E.Median	2.914	3.592	3.91	3.965	3.836	3.958

DocuSign Envelope ID: FF917FA4-BEA0-4E08-96D0-A9016C337F14

US 18 Raw Data	Normal_1	Normal_2	Normal_3	Muller_1	Muller_2	Muller_3
Width.V.Max	5.179	5.037	4.034	3.446	4.117	4.557
Width.V.P75	5.059	4.442	3.959	3.409	3.918	4.468
Width.V.Mean	4.734914894	4.413854167	3.876354167	3.142270833	3.9104375	4.319408163
Width.V.P25	4.382	4.351	3.812	2.954	3.885	4.276
Width.V.Min	4.193	4.276	3.687	2.785	3.832	3.843
Width.V.Median	4.748	4.413	3.875	3.015	3.902	4.434
Width.O.Max	3.862	4.083	4.46	2.921	3.662	4.071
Width.O.P75	3.67	3.993	4.413	2.858	3.603	4.013
Width.O.Mean	3.524595745	3.791553191	4.334020833	2.649489362	3.511617021	3.818833333
Width.O.P25	3.325	3.706	4.268	2.414	3.487	3.64
Width.O.Min	3.227	3.206	4.059	2.148	3.163	3.445
Width.O.Median	3.526	3.88	4.384	2.732	3.56	3.873
Width.T.Max	3.547	3.734	3.735	2.314	4.014	3.622
Width.T.P75	3.36	3.719	3.639	2.284	3.737	3.588
Width.T.Mean	3.211404255	3.555106383	3.498895833	2.232042553	3.525085106	3.394958333
Width.T.P25	3.1	3.368	3.348	2.182	3.377	3.389
Width.T.Min	3.08	2.667	3.256	2.072	2.683	2.764
Width.T.Median	3.118	3.705	3.508	2.244	3.521	3.471
Width.E.Max	2.834	3.515	3.329	3.057	3.993	4.137
Width.E.P75	2.721	3.509	2.817	2.897	2.976	3.676
Width.E.Mean	2.594695652	3.456468085	2.807617021	2.496553191	2.812702128	3.091791667
Width.E.P25	2.501	3.428	2.7	2.012	2.391	2.799
Width.E.Min	2.419	3.344	2.624	1.869	2.064	2.417
Width.E.Median	2.572	3.464	2.733	2.722	2.918	2.865